| OF |
AD—
A075557

Report No. 5210569

LEVEL

SUMMARY REPORT

PHASE II

AD**A075557**

REVERBERATION SPECTRUM PREDICTION MODEL

VOLUME 1

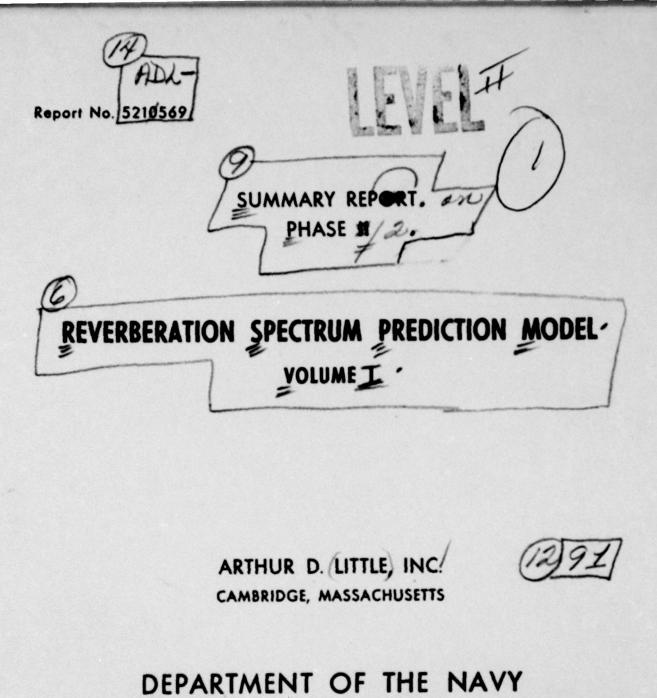**ARTHUR D. LITTLE, INC.**
CAMBRIDGE, MASSACHUSETTS

DDC

OCT 22 1978

A

DEPARTMENT OF THE NAVY
UNDERWATER SOUND LABORATORY

N00140-67-C-0265

79 10 22 046

MAY 1969

Report No. 5210569

(14) ADL-

LEVEL II

(9) SUMMARY REPORT. on
PHASE II / 2.

(6)

REVERBERATION SPECTRUM PREDICTION MODEL

VOLUME I

ARTHUR D. LITTLE, INC.
CAMBRIDGE, MASSACHUSETTS

(12) 91

DEPARTMENT OF THE NAVY
UNDERWATER SOUND LABORATORY

(15) new) NØØ140-67-C-0265

DDC
RECEIVED
OCT 22 1979
A

(11) MAY 1969

78 06 23 043
208850

TABLE OF CONTENTS:

i

Arthur D. Little, Inc.

ACKNOWLEDGMENTS

LIST OF FIGURES

LIST OF FIGURES (CONTINUED)

CHAPTER I

THE REVERBERATION MODEL

I. INTRODUCTION

In order to predict the performance characteristics of an active
sonar in a particular ocean environment one needs a certain amount of
knowledge concerning the nature of the background interference. Since
reverberation is a prime source of interference and since it is also a
random process, the theoretical description must be in terms of co-
variances, joint probability densities and other such probabilistic
quantities. The following sections develop one possible description
of the reverberation in these statistical terms.

Before beginning the detailed description of reverberation it is
advisable to consider briefly the assumptions which are used in this
description. The first is that the reverberation noise can be ade-
quately specified for engineering purposes by knowledge of the covariance
function only. The implication of this assumption is that a knowledge
of the covariance and corresponding power density spectrum is sufficient
for both engineering purposes and investigations of the statistical
nature of the reverberation noise amplitude. The second assumption is
that the properties of the various scattering media present in the ocean
are adequately described by the various experimental results reported in
the literature. Finally, it is assumed that the Fraunhofer diffraction
model used to characterize array patterns and the ray tracing method
for calculation of the geometrical propagation loss are both valid

approximations for the purposes of the reverberation description. The next step is to outline the method by which the covariance of the reverberation process is obtained.

II. THE COVARIANCE FUNCTION

1. Preliminary Remarks

The primary emphasis in the following sections will be placed on finding the covariance function resulting from scattering from a deep scattering layer. The results thus obtained for volume scattering can then be easily extended to the case of surface and bottom scattering.

The method used to obtain the covariance function may be outlined as follows:

a. The transmitted signal is first written in terms of its time and spatial dependence utilizing the Fraunhofer Diffraction model for the array and the geometrical spreading loss expression from Chapter II.

b. The interaction of the outbound pressure wave with the individual scatterers is evaluated utilizing the simplest scattering model which will give results consistent with the measured results.

c. The returning waves from all scatterers are then summed at the receiving array, after correction for its directional characteristics. The result is an equivalent noise voltage containing certain random parameters.

d. The next step involves writing the covariance function for the reverberation noise voltage, taking the required statistical averages, and then simplifying the resulting integrals.

e. The final step is to obtain the Fourier transform of the covariance function which represents the instantaneous power density spectrum of the reverberation noise.

During the course of the derivation outlined above certain mathematical difficulties do arise. In order to obtain a useful model these difficulties must be circumvented by judicious approximations. The most significant approximation is implicit in the above outline and involves the fact that the reverberation noise is in reality a non-stationary random process. A non-stationary random process is one for which the covariance function is time dependent. In general, such processes are analytically difficult to treat; however, there is one approximation which, if justified, greatly reduces the mathematical complexity of the problem. In particular, if it can be shown that the random waveform in question, say $r(t)$, can be factored into two parts as

$$r(t) = g(t) \, n(t) \tag{1}$$

in which $g(t)$ is a slowly varying totally deterministic function and $n(t)$ contains all of the remaining random parameters then the covariance of $r(t)$ may be obtained as follows. The true covariance is written as

$$R_{rr}(t,\tau) = \overline{r(t)\ r(t+\tau)} \qquad (2)$$

in which the horizontal bar indicates a statistical average over all random parameters in $r(t)$. Using the fact that $r(t)$ is factorizable the covariance may be written as

$$R_{rr}(t,\tau) = \overline{g(t)\ n(t)\ g(t+\tau)\ n(t+\tau)} \ . \qquad (3)$$

Since $g(t)$ contains no random parameters it may be brought outside of the expected value operation and $R_{nn}(t,\tau)$ becomes

$$R_{rr}(t,\tau) = g(t)\ g(t+\tau)\ \overline{n(t)\ n(t+\tau)} \ . \qquad (4)$$

Now, if $g(t)$ is a slowly changing function of time with regard to the covariance function of $n(t)$ alone, i.e.,

$$g(t) - g(t+\tau) << \overline{n(t)^2} - \overline{n(t)\ n(t+\tau)} \qquad (5)$$

then for a given instant of time, t_o, the true covariance function is closely approximated by

$$R_{nn}(t_o,\tau) \simeq [g(t_o)]^2\ \overline{n(t_o)\ n(t_o+\tau)} \qquad (6)$$

For the case of active sonar reverberation the approximation of equation (6) is reasonable provided that the transmitted signal pulse resolution length is small compared to the propagation range corresponding to the time t_o. The above considerations are shown in the form of a block diagram of the calculations in Figure I-1.

I-4
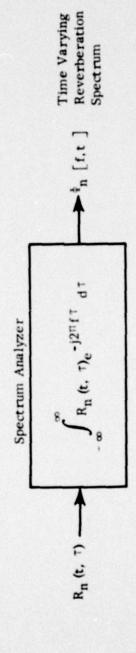
FIGURE I-1   BLOCK DIAGRAM OF THE REVERBERATION MODEL

Transmitted Signal s(t) → Reverberation Generator (Time Varying Linear System with Random Parameters) → n(t) → Correlator $\overline{n(t)\,n(t+\tau)}$ → Covariance Function $R_n(t,\tau)$

$R_n(t,\tau)$ → Spectrum Analyzer $\int_{-\infty}^{\infty} R_n(t,\tau)e^{-j2\pi f\tau}\,d\tau$ → $\phi_n[f,t]$ Time Varying Reverberation Spectrum

2. Propagation Loss

The following model which is derived in Chapter II is used to calculate the geometrical spreading loss along a ray path. The loss is given by

$$\frac{I}{I_o} = L(\phi_o) = \frac{r_o^2 \cos \phi_o}{x \left| \frac{\partial x}{\partial \phi_o} \right|_z \sin \phi_1} \tag{7}$$

where
- I_o is the initial intensity
- r_o^2 is a unit distance from the source, usually 1 yd
- ϕ_o is the initial ray angle
- ϕ_1 is the final ray angle
- x is the horizontal distance

In addition, with reference to Figure I-2 the following results for incremental volume and incremental area are noted.

$$\Delta V = x \left| \frac{\partial x}{\partial \phi_o} \right|_z \sin \phi_1 \; \Delta\theta \Delta\phi_o \Delta\delta \tag{8}$$

$$\Delta A = x \left| \frac{\partial x}{\partial \phi_o} \right| \Delta\theta \Delta\phi_o \tag{9}$$
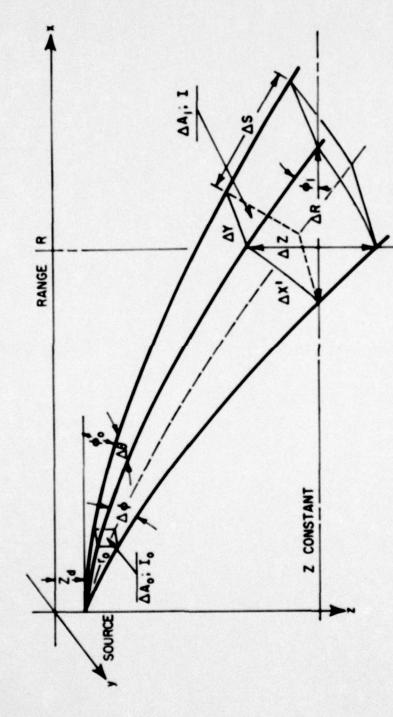
FIGURE I-2   PERTAINING TO THE EVALUATION OF THE TRANSMISSION LOSS

I-7

Arthur D. Little, Inc.

3. The Scattering Model

The ocean scattering model used in this derivation is made up of three principal scattering regions as shown in Figure I-3. The distribution of scatterers on the surface and bottom and within the deep scattering layer is assumed to be uniform with the following densities:

K_b = average number of scatterers per unit bottom area

K_s = average number of scatterers per unit surface area

K_v = average number of scatterers per unit volume within the deep scattering layer.

The basic model for the individual scatterers in each region is described by the following assumptions:

a. An individual scatterer is characterized by a complex scattering amplitude, $\widetilde{Z}_{ijk}$, which contains both the magnitude and phase information for the scattered wave. The subscripts refer to the physical location of the scatterer.

b. The expected value of the complex scattering amplitude is zero:

$$E\left[Z_{ijk}\right] = 0 \tag{10}$$

c. The returning waveforms from two scatterers located at different points in the ocean are uncorrelated. Thus

$$E\left[\widetilde{Z}_{ijk}\,\widetilde{Z}^{*}_{lmn}\right] = 0 \tag{11}$$

I-8

UNIFORM DISTRIBUTION OF SURFACE SCATTERERS OVER THE OCEAN SURFACE.

UNIFORM DISTRIBUTION OF VOLUMN SCATTERERS WITHIN A SCATTERING LAYER.

UNIFORM DISTRIBUTION OF BOTTOM SCATTERERS OVER THE OCEAN BOTTOM.

FIGURE I-3   SCATTERING REGIONS IN THE OCEAN MODEL

I-9

d. Due to the motion of scatterers on both the ocean surface and within the scattering layer there will be a Doppler shift associated with each scatterer. This Doppler shift will be a random variable and its effect on the returned waveform will be multiplication by a factor of the form

$$e^{j2\pi f_d(ijk)t}$$

These properties are illustrated in Figure I-4.

As for the gross effects of the scatterers such as mean scattered intensity and dependence on angle of incidence, it will be assumed that these characteristics are suitably accounted for by the following models:

a. For surface scattering the Chapman and Harris[1] surface scattering model is used. This model predicts that the average scattering level is

$$10 \log A_s = 3.3 \beta \log \frac{\emptyset_1}{30} - 42.2 \log \beta + 2.6 \qquad (12)$$

where

$$\beta = 158 \left[V_w f^{1/3} \right]^{-0.58}$$

and

$\emptyset_1$ = grazing angle in degrees

V_w = wind speed in knts

f = frequency in cps

A complete description of this model may be found in reference 1.

---

(1) Chapman, R. P. and Harris, J. H., "Surface Backscattering Strength Measured with Explosive Sound Sources." Defense Research Board, Naval Research Establishment, Canada, NRE Report 62/3. (UNCLASSIFIED)

Arthur D. Little, Inc.

x

INCOMING WAVE OF KNOWN MAGNITUDE
AND PHASE

RANDOM SCATTERING BODY
LOCATED AT θ_i, ϕ_j, S_k,
WITH SCATTERING AMPLITUDE
$\tilde{Z}_{ijk} = |Z_{ijk}| e^{jz_{ijk}}$

θ_i

ϕ_j

S_k

TRANSDUCER

SCATTERED WAVE OF
UNKNOWN MAGNITUDE
AND PHASE

z

y

FIGURE I-4   CHARACTERIZATION OF A SINGLE SCATTERER

I-11

b. The bottom scattering model is given by

$$10 \log A_B = -28 + 10 \log \sin \text{(grazing angle)} \qquad (13)$$
$$+ 10 \log \sin \text{(scattering angle)}$$

c. The volume scattering model assumes no dependence on incident angle and is characterized by a single constant. For the purposes of calculating predicted reverberation a mean square scattering strength of 10^{-7} per cubic yard was assumed.

4. The Covariance Function

The transmitted signal will have both a temporal and spatial dependency. In particular, if the velocity excitation applied to each transducer is

$$V(t) = \text{Re} \left[\tilde{v}(t) \, e^{j2\pi f_c} \right] \tag{14}$$

where $\text{Re}[\ ]$ indicates the real part of the quantity in brackets, then the corresponding pressure excitation as seen at some point in the far field of the transducer may be written as

$$\tilde{p}(t, \Theta_i, \emptyset_j, s_k) = \frac{a\rho c}{s_k} \, \tilde{v}\left(t - \frac{s_k}{c}\right)$$

$$\times \sum_{n=1}^{N} \exp j\left[\beta_n - \frac{2\pi}{\lambda}(\bar{\ell} \cdot \overline{r_n})\right] \tag{15}$$

The parameters in equation (25) are

$\Theta_i, \emptyset_j, s_k$ = observation corrdinates

ρ = density of seawater

c = Propagation velocity

s_k = propagation path length

β_n = arbitrary phasing of the nth transducer

λ = wavelength

$\bar{\ell}$ = unit direction vector

$\overline{r_n}$ = location vector of the nth transducer

a = a constant related to the particular transducer type

N = number of elements in the transducer

I-13

Equation (15) represents the result of doing a straightforward Fraunhofer diffraction calculation on the particular array in question. The physical situation is shown in Figure I-5. Equation (15) may be immediately simplified by noticing that the Fraunhofer diffraction pattern is independent of the excitation waveform so long as the waveform is the same for each element with the exception of phase. In this case, equation (15) may be written as

$$\widetilde{p} \ (t, \ \Theta_i, \ \emptyset_j, \ s_k) = \widetilde{v} \ (t - \frac{s_k}{c}) \ \widetilde{Q}_T \ [\Theta_i, \ \emptyset_j] \times L[0_h]^{\frac{1}{2}} \tag{16}$$

where

$$\widetilde{Q}_T \ [\Theta_i, \ \emptyset_j] = a\rho c \sum_{n=1}^{N} \exp j \ [\beta_n - \frac{2\pi}{\lambda} \ (\overline{l} \cdot \overline{r_n}) \ ]$$
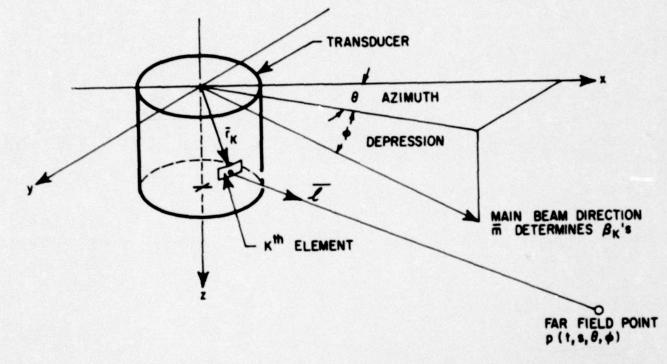
and the equation has been generalized to include propagation in a non-homogeneous medium by the addition of the loss term $L[\emptyset_j]$. One further generalization allows the consideration of rotating directional transmission in which case equation (16) becomes

$$\widetilde{p} \ (t, \ \Theta_i, \ \emptyset_j, \ s_k) = \widetilde{v} \ (t - \frac{s_k}{c}) \ \widetilde{Q}_T \ [\Theta_i - \Omega_o \ (t - \frac{s_k}{c}), \ \emptyset_j]$$

$$\times L[\emptyset_j]^{\frac{1}{2}} \tag{17}$$

where Ω_o is the rate of angular rotation of the beam.

Equation (17) may now be considered as the excitation applied to a scattering body located at Θ_i, $\emptyset_j$, s_k in which case the returning waveform is given by

I-14

TRANSDUCER

θ AZIMUTH

ϕ DEPRESSION

$\bar{r}_K$

$\bar{l}$

MAIN BEAM DIRECTION
$\bar{m}$ DETERMINES β_K's

K^{th} ELEMENT

FAR FIELD POINT
$p(t, s, \theta, \phi)$

SUMMATION OF CONTRIBUTIONS FROM ALL
ELEMENTS GIVES PRESSURE AS SEEN AT A
POINT (s, θ, ϕ) IN THE FAR FIELD

FIGURE I-5   INTERPRETATION OF THE FRAUNHOFER DIFFRACTION MODEL
FOR THE SPATIAL DEPENDENCE OF THE TRANSMITTED WAVEFORM

I-15

$$\tilde{p}(t, \Theta_i, \emptyset_j, s_k) = \tilde{Z}_{ijk} \, \tilde{v} \left(t - \frac{2s_k}{c}\right) \tilde{Q}_T \left[\Theta_i - \Omega_o \left(t - \frac{2s_k}{c}\right), \emptyset_j\right]$$

$$\times L[\emptyset_i]^{\frac{1}{2}} e^{-j2\pi \left[f_d(ijk) + f_s(\Theta_i, \emptyset_j)\right] t} \tag{18}$$

The last term in equation (18) contains two terms representing two distinct types of Doppler shift. The first type, $f_d(ijk)$, is the Doppler shift due to the scatterer motion and is a random variable. The second, $f_s(\Theta_i, \emptyset_j)$, represents the Doppler due to the motion of the source. In general, $f_s(\emptyset_i, \emptyset_j)$ is of the form

$$f_s(\Theta_i, \emptyset_j) = 2 \, f_c \left|\frac{v_s}{c}\right| \cos \Theta_i \cos \emptyset_j \tag{19}$$

where f_c is the carrier frequency and v_s is the ship velocity.

Considering equation (18) as a pressure excitation applied to the receiving array, the output noise voltage as seen at the receiver input may be written as

$$\tilde{n}(t) = \sum_i \sum_j \sum_k \tilde{Z}_{ijk} \, \tilde{v} \left(t - \frac{2s_k}{c}\right) \tilde{Q}_T \left[\Theta_i - \Omega_o \left(t - \frac{2s_k}{c}\right), \emptyset_j\right]$$

$$\times \tilde{Q}_R [\Theta_i, \emptyset_j] L[\emptyset_j] e^{-j2\pi \left[f_d(ijk) + f_s(\Theta_i, \emptyset_j)\right] t} \tag{20}$$

where $\tilde{Q}_R[\Theta_i, \emptyset_j]$ represents the receiving array characteristics and the result has been summed over all possible scattering bodies.

Having obtained an expression for the noise voltage the covariance function of $\tilde{n}(t)$ is obtained as follows. Equation (20) is entered into the defining equation for the covariance function to give

Arthur D. Little, Inc.

$$R_{nn}(t, t+\tau) = \tfrac{1}{2} \left\langle \widetilde{n}(t)\, \widetilde{n}^{*}(t+\tau) \right\rangle$$

$$= \tfrac{1}{2} \left\langle \sum_{ijk} \widetilde{Z}_{ijk}\, \widetilde{v}\left(t - \frac{2s_k}{c}\right) \widetilde{Q}_T\left[\Theta_i - \Omega_o\left(t - \frac{2s_k}{c}\right), \emptyset_j\right] \right.$$

$$\times\, \widetilde{Q}_R\left[\Theta_i, \emptyset_j\right] L\left[\emptyset_j\right] e^{-j2\pi\left[f_d(ijk) + f_s(\Theta_i, \emptyset_j)\right] t}$$

$$\times \sum_{\ell m n} \widetilde{Z}_{\ell m n}^{*}\, \widetilde{v}^{*}\left(t + \tau - \frac{2s_n}{c}\right) \widetilde{Q}_T^{*}\left[\Theta_\ell - \Omega_o\left(t + \tau - \frac{2s_n}{c}\right), \emptyset_j\right]$$

$$\times\, \widetilde{Q}_R^{*}\left[\Theta_\ell, \emptyset_m\right] L\left[\emptyset_m\right] e^{j2\pi\left[f_d(\ell,m,n) + f_s(\Theta_\ell, \emptyset_m)\right](t+\tau)} \left.\vphantom{\sum}\right\rangle \qquad (21)$$

where the symbols $\langle\ \rangle$ indicate an expected value operation.

The problem now is to accomplish a suitable simplification of equation (21). The first step in this simplification is to note that by the assumption of zero correlation between different scatterers the cross product terms in equation (21) must be zero. Thus, since

$$\left\langle \widetilde{Z}_{ijk}, \widetilde{Z}_{\ell m n}^{*} \right\rangle = 0 \qquad (11)$$

then

$$R_{nn}(t, t+\tau) = \tfrac{1}{2} \left\langle \sum_i \sum_j \sum_k \left|\widetilde{Z}_{ijk}\right|^2 \widetilde{v}\left(t - \frac{2s_k}{c}\right) \widetilde{v}^{*}\left(t + \tau - \frac{2s_k}{c}\right)\right.$$

$$\times\, \widetilde{Q}_T\left[\Theta_i - \Omega_o\left(t - \frac{2s_k}{c}\right), \emptyset_j\right] \widetilde{Q}_T^{*}\left[\Theta_i - \Omega_o\left(t + \tau - \frac{2s_k}{c}\right), \emptyset_j\right]$$

$$\times\, D_R\left[\Theta_i, \emptyset_j\right] L\left[\emptyset_j\right]^2 e^{j2\pi f_d(ijk)\,\tau}$$

$$\times\, e^{j2\pi f_s(\Theta_i, \emptyset_j)\,\tau} \left.\vphantom{\sum}\right\rangle \qquad (22)$$

The next step is to simplify the expression further by evaluating the required expected values. Now the only random parameters in equation (22) are the scattering amplitude and the scatterer doppler. Starting first with the scatterer doppler, the expected value of this quantity is written as

$$E\left[e^{j2\pi f_d(i, j, k)\tau}\right]$$

$$= 2\pi \int_{-\infty}^{\infty} e^{j2\pi f_d(ijk)\tau} p(2\pi f_d)df_d \tag{23}$$

where $p(2\pi f_d)$ is the probability density function for the Doppler shift of the scatterers. It is assumed to be the same for all scatterers within a particular scattering layer or on a particular scattering surface. The evaluation of equation (23) is particularly easy since its form corresponds directly to the form of the characteristic function of a probability density function. Thus

$$E\left[e^{j2\pi f_d(ijk)\tau}\right] = M(\tau) \tag{24}$$

where $M(\tau)$ is the characteristic function of $p[f_d(ijk)]$. From various experimental measurements[4] the form of $p[f_d(ijk)]$ has been found to be Gaussian to a reasonable approximation and hence

$$M(\tau) = e^{-\frac{1}{2}\sigma_d^2\tau^2} \tag{25}$$

where σ_d^2 is the variance of $p[f_d(ijk)]$. The range of σ_d^2 is between one and ten cycles per second for carrier frequencies from 3.5 to 5 kc and there is evidence that for surface reverberation σ_d^2 is a function of the angle of incidence of the excitation wave.

I-18

The second expected value operation to be performed is that pertinent to finding the mean square scattering strength. The required integral is written as

$$\overline{|\widetilde{z}_{ijk}|^2} = \int_{-\infty}^{\infty} |\widetilde{z}_{ijk}|^2 \, p_Z(\widetilde{z}_{ijk}) \, dZ \tag{26}$$

where $p_Z(\widetilde{z}_{ijk})$ represents the probability density function for the complex scattering amplitude. Since the scatterers are assumed to be localized to certain regions of the ocean the integral may be evaluated with the aid of Bayes' rule. Thus

$$p_Z(\widetilde{z}_{ijk}) = p_Z(\widetilde{z}_{ijk} | A \text{ scatterer}) \, P[\text{Scatterer}]$$

$$+ p_Z(\widetilde{z}_{ijk} | \text{No scatterer}) \, P[\text{No scatterer}] \tag{27}$$

If no scatterers are present, the scattering amplitude is zero with probability one and therefore the second term in equation (27) contributes nothing to the expected value integral. In the regions in which scatterers exixt the probability of finding a scatterer is

$$P[\text{Scatterer}] = K\Delta V \tag{28}$$

Using these results the mean square scattering strength is

$$\overline{|\widetilde{z}_{ijk}|^2} = K\Delta V \int_{-\infty}^{\infty} |\widetilde{z}_{ijk}|^2 \, p_Z(\widetilde{z}_{ijk}) \, dz_{ijk}$$

$$= KB_V \Delta V \tag{29}$$

where B_V is the mean square scattering strength per unit volume.

Inserting the results of equations (24) and (29) into equation (22) and using the expression

$$\Delta V = R \left| \frac{\partial R}{\partial \phi_o} \right| \sin \phi_o \, \Delta\theta \, \Delta\phi_o \, \Delta s \tag{8}$$

for the volume element gives

$$R_{nn}(t, \, t + \tau) = \frac{KB_V}{2} M(\tau) \sum_i \sum_j \sum_k \tilde{v} \left(t - \frac{2s_k}{c} \right) \tilde{v}^* \left(t + \tau - \frac{2s_k}{c} \right)$$

$$\times \tilde{Q}_T \left[\theta_i - \Omega_o \left(t - \frac{2s_k}{c} \right), \, \phi_j \right] \tilde{Q}_T^* \left[\theta_i - \Omega_o \left(t + \tau - \frac{2s_k}{c} \right), \, \phi_j \right]$$

$$\times D_R \left[\theta_i, \, \phi_j \right] L \left[\phi_j \right]^2 e^{j2\pi f_s(\theta_i, \phi_j)\tau}$$

$$\times R \left| \frac{\partial R}{\partial \phi_o} \right|_z \sin \phi_o \, \Delta\theta \, \Delta\phi_o \, \Delta s \tag{30}$$

Carrying the summations over into integrals gives

$$R_{nn}(t, \, t + \tau) = \frac{KB_V}{2} M(\tau) \int_o^{2\pi} d\theta \int_\phi d\phi \int_s \tilde{v}^* \left(t + \frac{2s}{c} \right) \tilde{v}^* \left(t + \tau - \frac{2s}{c} \right)$$

$$\times \tilde{Q}_T \left[\theta - \Omega_o \left(t - \frac{2s}{c} \right), \, \phi \right] \tilde{Q}_T^* \left[\theta - \Omega_o \left(t + \tau - \frac{2s}{c} \right), \, \phi \right]$$

$$\times D_R \left[\theta, \, \phi \right] L \left[\phi \right]^2 e^{j2\pi f_s(\theta, \phi)\tau}$$

$$\times R \left| \frac{\partial R}{\partial \phi_o} \right|_z \sin \phi_1 \, ds \tag{31}$$

Further simplification is obtained by noting that

$$L[\phi] \, R \left| \frac{\partial R}{\partial \phi_o} \right|_z \sin \phi_1 = r_o^2 \cos \phi_o \tag{32}$$

Hence, equation (31) may be written as

I-20

$$R_{nn}(t, t + \tau) = \frac{KB_v}{2} M(\tau) \int_0^{2\pi} d\Theta \int_\emptyset d\emptyset \int_s \tilde{v}\left(t - \frac{2s}{c}\right) \tilde{v}^*\left(t + \tau - \frac{2s}{c}\right)$$

$$\times \tilde{Q}_T\left[\Theta - \Omega_o\left(t - \frac{2s}{c}\right), \emptyset\right] \tilde{Q}_T^*\left[\Theta - \Omega_o\left(t + \tau - \frac{2s}{c}\right), \emptyset\right]$$
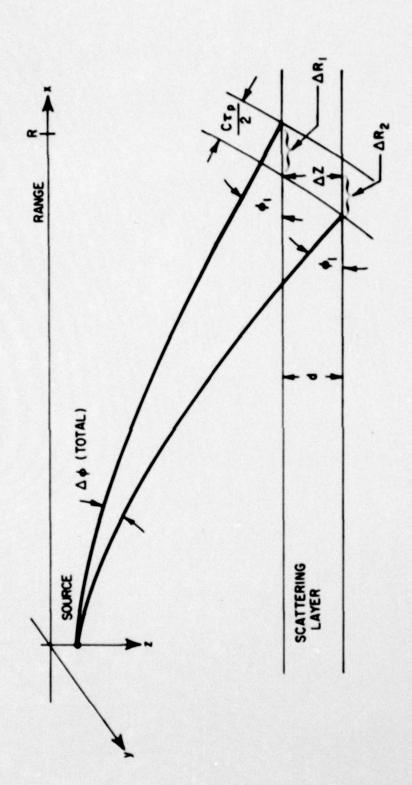
$$\times D_R[\Theta, \emptyset] \; L[\emptyset] \; r_o^2 \cos \emptyset_o \; ^{j2\pi f_s(\Theta, \emptyset)\tau} \; ds \qquad (33)$$

For the general case of time limited signals the integrals of equation (33) may be relatively easily evaluated. The factors which make this determination possible are first the spatial limitations on the distribution of scatterers, and second the spatial limitation on the ensonified regions at any given time due to the time limited nature of the signal. Both of these properties will be used to evaluate the integrals over $\emptyset$ and s.

The physical situation with regard to the scattering layer is shown in Fig. I-6. At any given instant of time, say t_o, the ensonified volume is limited by the upper and lower boundaries of the scattering layer and by the pulse resolution length. Since the individual scatterers are uncorrelated the integration over s must be zero for all s outside the ensonified region. As a consequence of this fact the integration over $\emptyset$ at the time, t_o, is limited to an integration over $\Delta\emptyset$ as defined by the boundaries of the ensonified volume.

To utilize the above results the integration on s is written as

FIGURE I-6   ENSONIFIED REGION OF THE SCATTERING LAYER PERTAINING TO THE EVALUATION OF $\Delta\phi$

$$\int_s \tilde{v}\left(t_o - \frac{2s}{c}\right) \tilde{v}^*\left(t_o + \tau - \frac{2s}{c}\right) \tilde{Q}_T\left[\theta - \Omega_o\left(t_o - \frac{2s}{c}\right), \phi\right]$$

$$\times \tilde{Q}_T^*\left[\theta - \Omega_o\left(t_o + \tau - \frac{2s}{c}\right), \phi\right] ds$$

$$= \int_s \tilde{g}\left[t_o - \frac{2s}{c}, \theta, \phi\right] \tilde{g}^*\left[t_o + \tau - \frac{2s}{c}, \theta, \phi\right] ds \qquad (34)$$

where

$$\tilde{g}\left[t_o - \frac{2s}{c}, \theta, \phi\right] = \tilde{v}\left(t_o - \frac{2s}{c}\right) \tilde{Q}_T\left[\theta - \Omega_o\left(t_o - \frac{2s}{c}\right), \phi\right]$$

Next a change of variable is made such that the integral becomes

$$\frac{c}{2} \int_\alpha \tilde{g}\left[t_o - \alpha, \theta, \phi\right] \tilde{g}^*\left[t_o + \tau - \alpha, \theta, \phi\right] d\alpha$$

$$= \frac{c}{2} R_{gg}(\tau, \theta, \phi) \qquad (35)$$

where $R_{gg}(\tau, \theta, \phi)$ is the correlation function of the transmitted signal including any effects due to rotating directional transmission.

For the case of fixed beam transmission the form of the complex directivity function for the transmitter $\tilde{Q}_T[\theta, \phi]$ is not dependent on time. In addition, the excitation signal $\tilde{v}(t)$ depends only on time. Thus, the quantity $R_{gg}(\tau, \theta, \phi)$ can be written in a factorized form as

$$R_{gg}(\tau, \theta, \phi) = \phi_{vv}(\tau) D_T[\theta, \phi] \qquad (36)$$

I-23

Using this result in equation (33) and assuming for the time being that rotating directional transmission is not used gives

$$R_{nn}(t, t + \tau) = A_v M(\tau) \, \emptyset_{vv}(\tau) \, r_o^2 \cos \emptyset_o$$

$$\frac{c}{2} \int_{\emptyset} L[\emptyset]d\emptyset \int_0^{2\pi} D_R(\Theta,\emptyset) \, D_T(\Theta,\emptyset) \exp{(j2\pi f_s(\Theta,\emptyset)\tau)}d\Theta \qquad (37)$$

where we have replaced the KB_v by an experimentally measured quantity A_v which we will call the scattering strength.

The most important terms in equation (37) from the standpoint of sonar design are the quantities $M(\tau)$, $\emptyset_{vv}(\tau)$ and the theta integration. As noted above the function $M(\tau)$ is simply the Fourier transform or characteristic function of the probability density function describing the random motion of the scatterers. In addition to the scatterer motion the function $M(\tau)$ can also be made to account for random motions of the transmitter and receiver. The overall effect of $M(\tau)$ is to introduce Doppler broadening to the reverberation return.

The correlation function of the transmitted signal, $\emptyset_{vv}(\tau)$, contains all of the information pertaining to the total energy and spectral content of the transmitted signal. For the purposes of this discussion the dimensions of $\emptyset_{vv}(\tau)$ will be watts per square centimeter.

The final term in equation (37) involves an integration over the azimuthal angle, Θ, of the receiver and transmitter directivity

functions and the exponential function containing the ships own Doppler expression. In general, this integral must be solved numerically because of the complicated form of the directivity function. The only exception to this is the case of omnidirectional transmission for which the directivity functions are unity for all θ and ϕ, in which case the integral reduces to a Bessel function multiplying the functions $M(\tau)$ and $\phi_{vv}(\tau)$. The significance of this integral lies in the fact that the ships own Doppler relation taken in conjunction with the directivity functions contributes to the Doppler spread of the reverberation.

The above considerations lead to the conclusion that the dimensions of the covariance function must be watts per square centimeters when the time shift τ is identically zero. Thus the total reverberation power being returned at a time, t_o, is just the evaluation of equation (37) with τ set to zero. The final step in the analysis is to obtain the spectral content of the reverberation by taking the Fourier transform of equation (37).

III. THE REVERBERATION SPECTRUM

The Fourier transform of $R_{nn}(t_o,\tau)$ is defined as

$$\phi_{nn}(t_o, f) = \int_{-\infty}^{\infty} R_{nn}(t_o,\tau) \, e^{-j2\pi f\tau} \, d\tau \tag{38}$$

where $\phi_{nn}(t_o,f)$ is interpreted as representing the distribution of the reverberation power as a function of frequency, f, at the time t_o. Inserting equation (37) for the covariance function gives

$$\phi_{nn}(t_o, f) = A_V V_o^2 \cos \phi_o \; \frac{c}{2} \int_\phi L[\phi] \, d\phi \int_0^{2\pi} D_T(\Theta,\phi) \, D_R(\Theta,\phi) \, d\Theta$$

$$\int_{-\infty}^{\infty} M(\tau) \, \phi_{vv}(\tau) \, e^{-J2\pi[f \,-\, f_s(\Theta,\phi)]\tau} \, d\tau \tag{39}$$

The final integral over τ is simply the Fourier transform of the product of two time functions which is simply the convolution of their respective Fourier transforms. Hence,

$$\phi_{nn}(t_o, f) = A_V \, r^2 \cos \phi_o \int_\phi L[\phi] \, d\phi \int_0^{2\pi} D_T(\Theta,\phi) \, D_R(\Theta,\phi) \, d\Theta$$

$$\int_{-\infty}^{\infty} F_M(\sigma) \, \phi_{vv}(f \,-\, f_s(\Theta,\phi) \,-\, \sigma) \, d\sigma \tag{40}$$

where $F_M(\sigma)$ is the Fourier transform of $M(\tau)$ and σ is a dummy variable of integration.

So far the discussion has been limited to scattering from a deep scattering layer; however, it should be pointed out that scattering from the ocean surface and the ocean bottom may be characterized by precisely the same techniques as were used to characterize the volume scattering problem. The answers are in fact identical in form and differ only in terms of the scattering coefficient and the scatterer dispersion functions. In addition, it is noted that the Fourier transform of the transmitted signal autocorrelation function may be written as

$$\phi_{vv}[f] = I_o \, \tau_p \, \Lambda[f] \tag{41}$$

I-26

where I_o is the peak transmitted intensity and τ_p the pulse length.
Thus, the product $I_o \tau_p$ contains the information as to the transmitted
energy and $\Lambda[f]$ gives the appropriate spectral distribution. In the
following section a complete summary of the reverberation equations is
given, including the substitution indicated by equation (41).

IV. SUMMARY OF THE REVERBERATION EQUATIONS FOR FIXED BEAM TRANSMISSION

a. List of Quantities

1) I_o ; Peak transmitted intensity in watts per square centimeter

2) τ_p ; Pulse length in seconds

3) A_v ; Volume scattering strength per cubic yard

4) A_B ; Bottom scattering strength per square yard

5) A_s ; Surface scattering strength per square yard

6) c ; Velocity of propagation

7) r_o ; Unit distance of one yard

8) ϕ_1 ; Angle of incidence of wavefront with scattering surface or volume

9) $f_s(\theta, \phi)$; Ship's own Doppler function

10) ϕ_o ; Initial angle at the transmitter for the ray which strikes a scattering boundary at time $\frac{1}{2}t_o$

11) t_o ; Round trip travel time for the reverberation components

12) $L[\phi]$; Geometrical-spreading component of intensity loss (one way)

13) f ; Frequency in c.p.s.

14) $D_T[\theta, \phi]$ and $D_R[\theta, \phi]$; Transmitting and receiving directivity functions, respectively

15) $M(\tau)$; Scatterer dispersion function relating to random motion of the scatterers

16) $F_M(\sigma)$; The Fourier transform of $M(\tau)$

17) $\phi_{vv}(\tau)$; Autocorrelation function of the transmitted waveform

18) $\Lambda[f]$; Spectral distribution function for the energy in the transmitted waveform

b. Reverberation Equations

The covariance function is given by

$$R_{nv}(t_o, \tau) = A_v \, r_o^2 \, \cos \phi_o \, \frac{1}{2} \, M_v(\tau) \, \phi_{vv}(\tau)$$

$$\times \int_\phi L\,[\phi] \, d\phi \int_0^{2\pi} D_T(\theta, \phi) \, D_R(\theta, \phi) \, e^{j2\pi f_s(\theta, \phi)\tau} \, d\theta \qquad (42)$$

and the power density spectrum,

$$\phi_{nv}(t_o, f) = A_v \, r_o^2 \, \cos \phi_o \, I_o \, \frac{c\tau_R}{2} \int_\phi L[\phi] \, d\phi$$

$$\times \int_0^{2\pi} D_T(\theta, \phi) \, D_R(\theta, \phi) \, d\theta \int_{-\infty}^{\infty} F_M(\sigma) \phi_{vv}(f - f_s(\theta, \phi) - \sigma) \, d\sigma \qquad (43)$$

The only significant differences betweeen the various types of reverberation, surface volume or bottom, aside from their respective scattering models is the effect form of the characteristic function $F_M(\sigma)$. For the purposes of general systems analysis application, the assumption of a gaussian form for $F_M(\sigma)$ is reasonable in view of the existing experimental data.

I-29

V.   THE EVALUATION OF THE REVERBERATION EQUATIONS

The numerical evaluation of the reverberation equation begins with an algorithm named TIMBR whose purpose is to characterize a particular ocean environment in terms of the initial ray angles required to propagate a ray to a predetermined point in both space and time. The details of this algorithm are given in Chapter IV. The basic method used by the TIMBR algorithm is essentially an exhaustive characterization in which rays are traced from a source over a very wide aperture and out to propagation times equal to or greater than the maximum reverberation time of interest. A reasonably fine grid of initial angles is used to cover the aperture and the ray parameters such as range and depth are recorded at regular time intervals as the rays are traced. This results in the creation of a number of TIMBR arrays and corresponding to a particular time and containing all of the ray parameters for that time for all of the rays in the aperture. Thus timer provides the ray parameters such as range and depth both as tabulated functions of initial angle and as tabulated functions of time. Having obtained the TIMBR description of the particular ocean environment it is then possible to interpolate in the TIMBR tables by the method described in Chapter IV to obtain the integration ranges over the variable $\emptyset$ to be used in evaluating equation (43). In addition, the initial angles to be used in the evaluation of the propagation loss are also made available.

Given that the initial ray angles and depression angle $\emptyset$ integration range have been determined, the next step is the evaluation of the innermost signal convolution integral which is accomplished by means

of the fast Fourier transform as described in Chapter V. The next integral is in azimuth over the transducer and receiver arrays and is by far the most time-consuming since the array directivity must be calculated by the Fraunhofer diffraction method once for each step of the integral. Finally, the integration over depression angle ϕ is performed to give the reverberation spectrum at a given time.

The remaining chapters give complete details of the methods of performing each of the calculations listed above.

CHAPTER II

GEOMETRICAL SPREADING LOSS - GENERAL

The spreading loss along a ray path may be obtained by considering the variation in energy density in a ray bundle centered on the ray path. There are two ways by which this may be accomplished. First, consider the situation shown in Fig. II-1 for which the power leaving the source through area A_o is given by

$$P_o = I_o A_o \tag{1}$$

where I_o is the initial intensity at a distance, r_o, from the source. At some distant point, x_1, z_1, the intensity is I_1 over an area A_1 such that

$$P_o = I_o A_o = I_1 A_1 \tag{2}$$

which leads to the spreading loss

$$L = \frac{I_1}{I_o} = \frac{A_o}{A_1} \tag{3}$$

From Fig. II-1 note that A_o is given by

$$A_o = r_o^2 \cos \phi_o \, \Delta\phi_o \, \Delta\theta \tag{4}$$

where ϕ_o is the initial depression angle. The area A_1 at x_1, z_1 is given by

$$A_1 = hw = x_1 \Delta\theta \, \Delta x \, \sin\phi_1 \tag{5}$$

II-1

Thus the ratio of A_o to A_1 in Equation 3 is

$$\frac{A_o}{A_1} = \frac{r_o^2 \cos\phi_o \, \Delta\phi_o \, \Delta\theta}{x_1 \, \Delta\theta \, \Delta x \, \sin\phi_1} \tag{6}$$

which in the limit as $\Delta\phi_o \to 0$ becomes

$$L = \frac{r_o^2 \cos\phi_o}{x \left|\frac{\partial x}{\partial\phi_o}\right|_z \left|\sin\phi_1\right|} \tag{7}$$

Equation 7 is perfectly general in that no assumptions have been made concerning the velocity profile. However, if the velocity profile is linear, then the rays are known to be arcs of circles and the partial derivative $\left|\partial x/\partial\phi_o\right|_z$ can be evaluated as follows. For the straight line velocity profile with gradient g, the horizontal distance x is given by

$$x = \int_{s_1}^{s_2} \cos\phi \, ds = -\int_{\phi_o}^{\phi_1} \cdot \frac{\cos\phi}{gp} \, d\phi = -\frac{1}{gp} \sin\phi \Big|_{\phi_o}^{\phi_1}$$

$$= \frac{1}{gp} (\sin\phi_1 - \sin\phi_o) \tag{8}$$

where $p = \frac{\cos\phi}{c} = \frac{\cos\phi_o}{co}$ and is constant for a ray in a constant velocity gradient, as a consequence of Snell's law.

II-2

Differentiating Equation 8 gives

$$\frac{\partial x}{\partial \phi_o} = \frac{\partial}{\partial \phi_o} \left[\frac{c_o}{g \cos\phi_o} (\sin\phi_1 - \sin\phi_o) \right]$$

$$\text{(9)}$$

$$= \frac{c_o}{g^2 \cos^2\phi_o} \left[\left(\cos\phi \frac{\partial \phi_1}{\partial \phi_o} - \cos\phi_o\right) g \cos\phi_o + (\sin\phi_1 - \sin\phi_o) g \sin\phi_o \right]$$

The term $\partial \phi / \partial \phi_o$ is obtained from

$$\phi = \cos^{-1} \frac{c(z) \cos\phi_o}{c_o}$$

$$\frac{\partial \phi}{\partial \phi_o} = \frac{\sin\phi_o}{\sqrt{1 - \frac{c(z)^2 \cos^2\phi_o}{c_o^2}}} \cdot \frac{c(z)}{c_o} = \frac{c(z)}{c_o} \frac{\sin\phi_o}{\sin\phi}$$

but

$$\frac{c(z)}{c_o} = \frac{\cos\phi}{\cos\phi_o}$$

from which

$$\frac{\partial \phi}{\partial \phi_o} = \frac{\cos\phi \sin\phi_o}{\cos\phi_o \sin\phi}$$

$$\text{(10)}$$

Using this result in Equation 9 gives

$$\frac{\partial x}{\partial \phi_o}\bigg|_z = \frac{c_o}{g \cos^2\phi_o \sin\phi} \left[\sin\phi_o - \sin\phi\right]$$

$$= -\frac{x}{\cos\phi_o \sin\phi} \tag{11}$$

Using this result in Equation 7 gives for the spreading loss

$$L = \frac{I_1}{I_o} = \frac{r_o^2 \cos^2\phi_o}{x^2} \tag{12}$$

This expression is valid until the ray reaches a boundary between zones of different velocity gradient.

The effect of the change in velocity gradient at a zone boundary is accounted for in the following manner. With reference to Fig. II-2, Equation 7 becomes

$$L = \frac{I}{I_o} = \frac{r_o^2 \cos\phi_o}{x \left|\frac{\partial}{\partial \phi_o} (x_1 + (x_2 - x_1) + (x - x_3))\right| \sin\phi} \tag{13}$$

In general for any point in the $(n+1)^{th}$ velocity profile zone,

$$x - x_n = \frac{c_o}{\cos\phi_o \, g_{n+1}} (\sin\phi_n - \sin\phi) \tag{14}$$
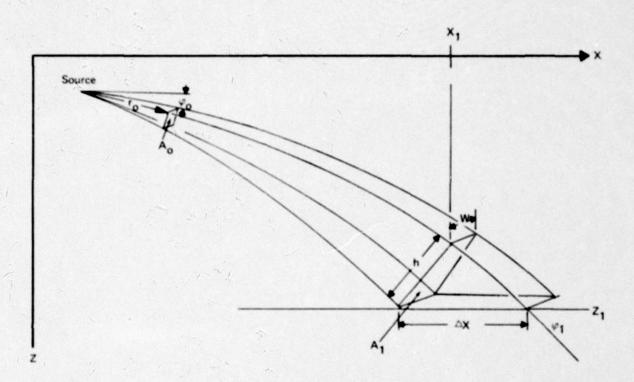
II-4

FIGURE II–1   GEOMETRY PERTAINING TO THE CALCULATION OF SPREADING LOSS

Differentiating with respect to ϕ_0

$$\frac{\partial}{\partial \phi_0} (x-x_n) = \frac{c_0}{\cos^2 \phi_0 \, g_{n+1}} \left[\cos\phi_0 \left(\cos\phi_n \frac{\partial \phi_n}{\partial \phi_0} - \cos\phi \frac{\partial \phi}{\partial \phi_0} \right) \right.$$

$$\left. + \sin\phi_0 \, (\sin\phi_n - \sin\phi) \right] \tag{15}$$

From Snell's law:

$$\frac{\partial}{\partial \phi_0} (\cos\phi) = \frac{c(z)}{c_0} \frac{\partial}{\partial \phi_0} \cos\phi_0$$

$$- \sin\phi \frac{\partial \phi}{\partial \phi_0} = - \frac{c(z)}{c_0} \sin\phi_0$$

$$\frac{\partial \phi}{\partial \phi_0} = \frac{\cos\phi}{\cos\phi_0} \frac{\sin\phi_0}{\sin\phi}$$

Using this result in Equation 15 gives

$$\frac{\partial}{\partial \phi_0} (x-x_n) = \frac{c_0}{\cos^2 \phi_0 \, g_{n+1}} \left[\frac{\cos^2 \phi_n \, \sin\phi_0}{\sin\phi_n} - \frac{\cos^2 \phi \, \sin\phi_0}{\sin\phi} \right.$$

$$\left. + \sin\phi_n \, \sin\phi_0 - \sin\phi \, \sin\phi_0 \right]$$

$$= - \frac{\sin\phi_0}{\cos\phi_0 \, \sin\phi \, \sin\phi_n} \frac{1}{p \, g_{n+1}} (\sin\phi_n - \sin\phi)$$

$$= - \frac{(x-x_n) \, \sin\phi_0}{\cos\phi_0 \, \sin\phi \, \sin\phi_n} \tag{16}$$
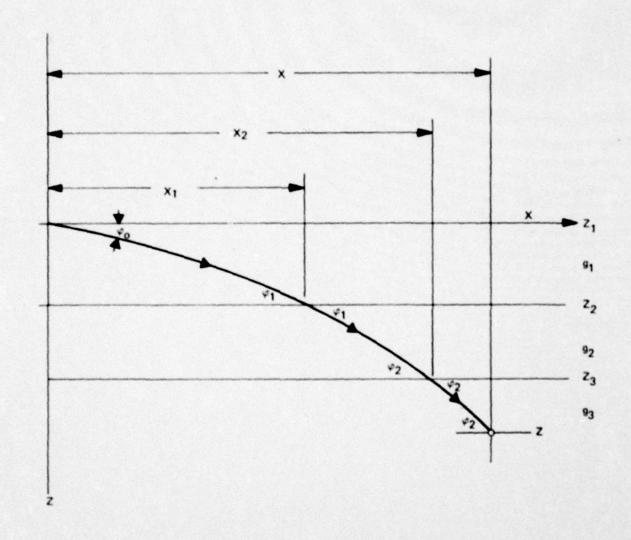
FIGURE II–2   PERTAINING TO THE CALCULATION OF REFRACTION LOSS IN A MULTI-LAYERED MEDIUM

Thus for the three layer case given in Equation 13,

$$L = \frac{I}{I_o} = \frac{r_o^2 \cos^2\phi_o}{x \left| \left[\frac{x_1}{\sin\phi_1} + \frac{(x_2-x_1)\sin\phi_o}{\sin\phi_2 \, \sin\phi_1} + \frac{(x-x_2)\sin\phi_o}{\sin\phi_2 \, \sin\phi} \right] \right| \, |\sin\phi|} \tag{17}$$

More generally for a ray traversing N zones with a terminal point in the $N+1^{th}$ zone

$$L = \frac{I}{I_o} = \frac{r_o^2 \cos^2\phi_o}{x \left| \left[\left(\sin\phi_o \sum_{n=1}^{N} \frac{(x_n-x_{n-1})}{\sin\phi_n \, \sin\phi_{n-1}} \right) + \frac{(x-x_N)\sin\phi_o}{\sin\phi_N \, \sin\phi} \right] \right| \, |\sin\phi|} \tag{18}$$

Finally, if a ray is specularly reflected from a plane surface, the reflection must be accounted for just as though a new zone had been entered. Fig. II-3 illustrates this case for surface reflection.

The refraction loss in the specular reflection case is calculated using

$$\frac{\partial x}{\partial \phi_o} = \frac{\partial}{\partial \phi_o} \left[\ldots (x_{n-1} - x_{n-2}) + (x_n - x_{n-1}) + (x_{n+1} - x_n) + \ldots \right]$$

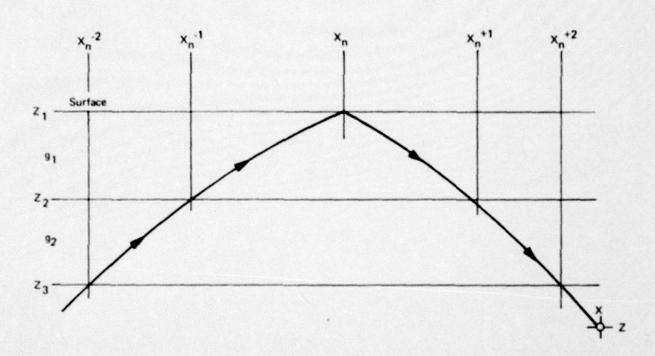just as though the ray were traversing multiple layers.

II-8

FIGURE II-3 REFRACTION LOSS IN THE SPECULAR REFLECTION CASE

CHAPTER III

DETAILS OF PROPAGATION LOSS CALCULATION

Total propagation loss for the selected rays consists of the spreading loss defined by equation (18) in Chapter II, plus attenuation, surface and bottom losses. Automation of the loss calculations requires consideration of various special cases, such as the tracing of vertexing rays. This chapter describes the methods used to deal with these situations. Details of the computer programs are contained in Volume II of this report.

1. Ray Tracing

The subroutine RAYTRK is used in both the TIMER and propagation loss calculations. It follows a ray leaving a starting point in some direction, until a specified amount of time has elapsed. TIMER allows the determination of the angles at which rays must leave the transmitter in order to terminate on surface, bottom or volume scatterers at a particular time. PLOSS repeats the ray trace for each of the selected initial angles and, in addition, develops all of the quantities necessary to evaluate equation (18) in Chapter II. The ray tracing is done in steps along the arc length, with the step size adjustable as critical points, such as vertices, zone boundaries and end times are approached. Newton's method is used to adjust the step size and direction in order to force the ray trace to converge on a specific point. The precision of convergence is a programmer controlled input.

III-1

The convergence scheme is tailored to the reverberation problem in the following manner. The objective is to terminate the ray at some specific time and, in particular, two of the three possible cases involve surface or bottom terminations. For these cases the program simply converges on the required number of surface or bottom bounces with no other test on propagation time. This approach is made possible because of the use of the TIMER algorithm which generates the appropriate initial conditions and gives the number of surface and bottom bounces required to achieve a surface or bottom termination at a predetermined time. The third type of convergence involves termination within a scattering layer at some specified time. This form of convergence uses Newton's method to obtain a final ray position.

In order to evaluate the propagation loss expression of equation (18) in Chapter II, it is necessary to know the complete history of the ray as it traverses each velocity profile zone. This history is generated by the ray tracing subroutine RAYTRK. The ray trace equations are obtained as follows.

The curvature of the ray is

$$\frac{d\phi}{ds} = - \cos\phi \, \frac{1}{c(z)} \cdot \frac{dc(z)}{dz} \tag{1}$$

where ϕ is the ray angle, s is the arc length, z the depth and $c(z)$ the velocity as a function of depth within the zone. For the case of constant gradients, $dc(z)/dz = g_k$ for the kth zone. Also since the gradient is constant in z, Snell's law holds and

Arthur D. Little, Inc.

$$\frac{\cos\phi}{c(z)} = \frac{\cos\phi_o}{c_o} = P_o \tag{2}$$

where c_o is the velocity at the source and ϕ_o is the initial angle. Thus the curvature may be written as

$$\frac{d\phi}{ds} = -g_k P_o = \frac{1}{R_k} \tag{3}$$

where R_k is the radius of curvature in the kth zone. Hereafter, the subscript k indicating the kth zone will be omitted, and it will be understood that all equations hold within one zone.

The horizontal distance travelled by the ray is given by *

$$x_2 - x_1 = \int_{\phi_1}^{\phi_2} \cos\phi \ ds \tag{4}$$

Using equation (3) to effect a change of variable, we obtain

$$x_2 - x_1 = -\frac{1}{gP} \int_{\phi_1}^{\phi_2} \cos\phi \ d\phi = -\frac{1}{gP} (\sin\phi_2 - \sin\phi_1)$$

$$= R (\sin\phi_2 - \sin\phi_1) \tag{5}$$

The vertical distance is given by

$$z_2 - z_1 = \int_{\phi_1}^{\phi_2} \sin\phi \ ds = -\frac{1}{gP} \int_{\phi_1}^{\phi_2} \sin\phi \ d\phi$$

$$= \frac{1}{gP} (\cos\phi_2 - \cos\phi_1) = -R (\cos\phi_2 - \cos\phi_1) \tag{6}$$

* In this and similar integrations, the integration is split into two parts whenever a ray vertexes.

III-3

Since the depth variable is used by the program as an independent variable, equation (6) provides a means of obtaining the final angle as follows:

$$\phi_2 = \left\{ \cos^{-1} \left(\cos\phi_1 - \frac{z_2 - z_1}{R} \right) \right\} \cdot \rho \tag{7}$$

where ρ is either ± 1 and is used to assign the appropriate sign to the final angle ϕ_2. The method of choosing ρ will be discussed when we consider the detailed application of the above equations.

The arc length s is given by

$$s_2 - s_1 = \int_{\phi_1}^{\phi_2} \frac{dz}{\sin\phi} = \int_{\phi_1}^{\phi_2} \frac{dz}{\sqrt{1 - \cos^2\phi}} \tag{8}$$

Using Snell's Law and equation (3), note that

$$\cos^2\phi = c(z)^2 p_o^2 \tag{9}$$

and

$$dz = \frac{1}{p_o g} \, d(c(z)p_o) \tag{10}$$

Inserting these results in equation (8) gives

$$s_2 - s_1 = \frac{1}{g p_o} \int_{z_1}^{z_2} \frac{d(c(z)p_o)}{\sqrt{1 - c(z)^2 p_o^2}}$$

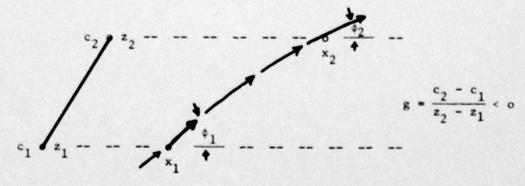$$= - R \left[\sin^{-1} c(z_2)p_o - \sin^{-1} c(z_1)p_o \right] \cdot \rho \tag{11}$$

III-4

The detailed application of these equations requires consideration of four possible cases as illustrated below. For the two cases involving vertexing rays, the calculations are done from the initial point to the vertex point with complete evaluation of all integrals. The ray is then traced from the vertex point to the next boundary. This procedure is required since the vertex point is a singular point and any attempt to simply integrate through this point will give erroneous results.

Case Ia   Gradient $< o$ Initial angle $< o$

Radius of curvature: $R = -\dfrac{1}{gP_o}$

$\therefore R > o$

Horizontal distance: $|\sin\phi_1| > |\sin\phi_2|$

$\therefore x_2 - x_1 > o$

Final angle: since $R > o$ and

$$z_2 - z_1 < o \quad \text{then} \quad -\frac{z_2 - z_1}{R} > o$$

$$\therefore \rho = -1$$

Arc length: $\sin^{-1}(c_1 p_o) < \sin^{-1}(c_2 p_o)$

$\therefore \rho = -1$ in order that $s_2 - s_1 > o$

$$g = \frac{c_2 - c_1}{z_2 - z_1} < o$$

NOTE: Had the vertex depth fallen in the above zone, it would have replaced z_2 as the upper boundary.

III-5

Case Ib   Gradient $< o$ Initial angle $> o$

Radius of curvature: $R = -\dfrac{1}{gP_o} > o$

Horizontal distance:
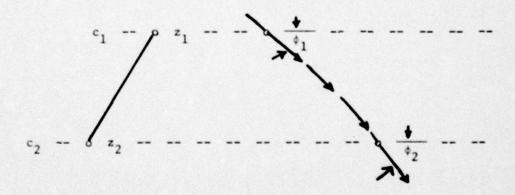
$$\sin\phi_1 < \sin\phi_2$$

$$\therefore x_2 - x_1 > o$$

Final angle: since $R > o$ and

$$z_2 - z_1 > o, \text{ then } -\frac{z_2 - z_1}{R} < o$$

$$\therefore \rho = +1$$

Arc length: $\sin^{-1} c_1 p_o > \sin^{-1} c_2 p_o \quad \therefore \rho = +1$

such that $s_2 - s_1 > o$

NOTE: Vertexing is not possible in this case.

Case IIa

Gradient > o   Initial angle > o

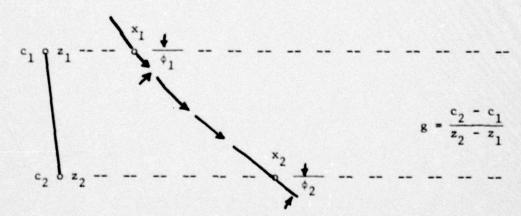Radius of curvature: $R = -\dfrac{1}{gP_o} < o$

Horizontal distance:

$$\sin\phi_1 > \sin\phi_2 \quad \therefore \; x_2 - x_1 > o$$

Final angle: since $R < o$ and

$$z_2 - z_1 > o, \text{ then } \quad -\dfrac{z_2 - z_1}{R} > o$$

and $\rho = +1$

Arc length: $\sin^{-1} c_1 p_o < \sin^{-1} c_2 p_o \quad \therefore \; \rho = +1$

such that $s_2 - s_1 > o$

$$g = \dfrac{c_2 - c_1}{z_2 - z_1}$$

NOTE: If the vertex depth were contained in this zone, it would have been used as the lower boundary.

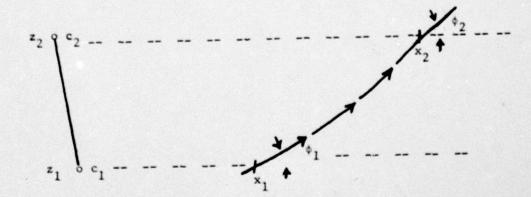Case IIb   Gradient > o   Initial angle < o

Radius of curvature: $R = -\dfrac{1}{gP_o} < o$

Horizontal distance:

$$|\sin\phi_1| < |\sin\phi_2| \quad \therefore \; x_2 - x_1 > o$$

Final angle: since $R < o$ and $z_2 - z_1 < o,$

$$\text{then} \quad -\frac{z_2 - z_1}{R} < o \quad \text{and} \quad \rho = -1$$

Arc length: $\sin^{-1} c_1 p_o > \sin^{-1} c_2 p_o \quad \therefore \; \rho = -1$

such that $s_2 - s_1 > o$

NOTE: Vertexing is not possible for this case.

The program differentiates between each of these four cases based on the gradient and initial angle at the starting point. The appropriate boundary is then established (vertex point or zone boundary) and the ray is traced to this boundary. All ray parameters are evaluated and a test for convergence is made. If the ray has not yet converged, the ray trace loop is repeated for the next zone.

When the ray has converged on the surface, bottom, or time specified, all of the parameters necessary for evaluation of equation (18) in Chapter II are saved for entry into subroutine PLOSS.

2. Propagation Loss

The propagation loss for a ray traversing N zone boundaries is given by

$$
L = \frac{r_o^2 \cos^2 \phi_o}{x \left| \left\{ \sin\phi_o \sum_{n=1}^{N} \frac{x_n - x_{n-1}}{\sin\phi_n \sin\phi_{n-1}} + \frac{(x-x_N) \sin\phi_o}{\sin\phi_N \sin\phi} \right\} \right| \cdot |\sin\phi|} \tag{12}
$$

where x_n and ϕ_n are the horizontal coordinate and final angle at each zone boundary as generated by RAYTRK; subroutine PLOSS is used to evaluate equation (12) at each zone boundary and at each convergence point. PLOSS also takes appropriate action for the following special cases.

a. If the ray starts with initial angle $\phi_o = 0$, then equation (12) indicates that all zones, except the zones in which the ray vertexes, will be characterized by the following propagation loss.

$$
L = \frac{r_o^2 \cos^2 \phi_o}{x \left| \frac{x_1}{\sin\phi_1} \right| |\sin\phi|} \tag{13}
$$

III-9

In a vertex zone equation (12) is valid until the ray actually reaches the vertex point at which point the intensity is indeed infinite. The subroutine tests the final angle PHI2 for zero and, if true, the loss is set equal to zero, and an indicator is set equal to indicate the infinity condition. Following the vertex, equation (13) is used until the next vertex point is reached.

b. For vertexing rays other than the ray with zero initial angle, we use the limiting form for the propagation loss as ϕ approaches zero which gives

$$L = \frac{r_o^2 \, \cos^2 \phi_o}{x \left| \dfrac{(x-x_N) \, \sin \phi_o}{\sin \phi_N} \right|} \tag{14}$$

The program makes the assumption that a ray will never be allowed to have a simultaneous vertex and zone transition, i.e., if the vertex depth and the zone depth are identical, then the ray is assumed to vertex in that zone.

At the conclusion of PLOSS the spreading loss has been computed for one of rays identified by TIMER. Additional subroutines are used to supply the corresponding surface, bottom and attenuation losses.

III-10

3. Absorption Loss

RAYTRK is capable of selecting from a set of four absorption models contained in subroutine AL1. The two models presently available are zero absorption and the Thorpe[1] model where

$$\text{ATLOSS} = \frac{0.1f^2}{1+f^2} + \frac{40f^2}{4100 + f^2} \quad \text{db/kyd}$$

with f = frequency in kilohertz

4. Bottom Loss

RAYTRK can call on subroutine BL1 for either zero loss or an acoustic province and incident angle dependent loss.

5. Surface Loss

RAYTRK has provision for a surface loss model through sub-routine SL1. At present this choice is limited to either zero or 3 db loss per bounce.

[1] Thorpe, W. H., Analytical Description of the Low Frequency Attenuation Coefficient, J. Acoustical Soc of America, Vol 42, No. 1, July 1967, p. 270.

CHAPTER IV

THE TIMER ALGORITHM

In Chapters II and III the mechanics of ray tracing and the calculation of propagation loss have been treated in some detail. This chapter will be concerned with the application of these calculations through the use of the TIMER algorithm to the evaluation of the reverberation equation.

The reverberation equation contains only two ray parameters explicitly, these being the round trip propagation time and the propagation loss along the round trip path. However, implicit in this equation is the assumption of spatial continuity of the round trip reverberation path. This assumption is of some practical importance when one attempts a numerical evaluation of the reverberation equation, since bistatic reverberation paths (i.e., paths for which the outbound and inbound ray paths are different) are, in many cases, quite significant. Thus we seek a method of characterizing each ocean environment to be investigated in a manner which will be consistent with the assumptions of spatial and temporal continuity. The TIMER algorithm meets these requirements, and its operation is described as follows.

1. First, consider the problem of evaluating the propagation time along a given ray path. In differential form we have

$$\frac{dt}{ds} = \frac{1}{c(z)} \tag{1}$$

IV-1

where t is time, s is arc length, and $c(z)$ is the propagation velocity along the ray path. Equation (1) is placed in a convenient form for integration by the following manipulations:

$$dt = \frac{dz}{c(z) \sin\phi} = \frac{dz}{c(z) \sqrt{1-\cos^2\phi}}$$

$$= \frac{dz}{c(z) \sqrt{1-c(z)^2 p^2}} \qquad (2)$$

where $\qquad p = \frac{\cos\phi}{c(z)} = \frac{\cos\phi_o}{c(z_o)}$, a constant for a given ray.

For the particular case in which $c(z)$ is a linear function in z, equation (2) may be integrated in closed form, since

$$c(z) = c_o + gz$$

$$\underline{\text{AND}} \qquad \frac{dc(z)}{dz} = g \qquad \underline{\text{OR}} \qquad dz = \frac{1}{g} dc(z)$$

from which

$$t_2 - t_1 = \frac{1}{g} \int_{z_1}^{z_2} \frac{dc(z)}{c(z) \sqrt{1-p^2 c^2}}$$

$$= -\frac{1}{g} \log_e \left[\frac{c_2}{c_1} \cdot \frac{1 + \sqrt{1-c_1^2 p^2}}{1 + \sqrt{1-c_2^2 p^2}} \right] \qquad (3)$$

where the variation in z from z_1 to z_2 is that encountered in traversing the ray path specified by p from s_1 to s_2. Implicit in this expression is the condition that the integration path may not pass through a vertex point, since the integrand is unbounded at such a point. However, the

IV-2

integral is convergent in the limit as the arc length approaches a vertex and hence, the integral may be evaluated in steps between each vertex. In addition, the sign to be used with the radical is determined by noting that

$$\sqrt{1 - c^2 p^2} = \sin\phi \tag{4}$$

where ϕ is the ray angle.

2. The basic method of applying equation (3) to the characterization of a given ocean environment starts by tracing from the source some large number of rays distributed in equal increments of initial angle. During the course of tracing each ray, the program stores the ray parameters at a set of predetermined times. These times usually correspond to the times at which reverberation spectra are to be evaluated. The convergence of each of the rays to the desired propagation time is accomplished by use of a Newton's method subroutine which provides numerical solution of equation (3) in terms of the ray depth z for each ray.

The result of this effort is a series of TIMER tables each corresponding to a given time and each containing a complete set of ray parameters for that propagation time. Thus, the individual TIMER tables constitute a description of the wave front at each specified time in terms of the initial ray angles. This feature of the TIMER tables allows their direct use in evaluating the reverberation equation, since the initial ray angle is in fact sufficient to completely describe the ray path.

To further illustrate this point consider the graph shown in Fig. IV-1. This particular graph is a plot of the TIMER data corresponding to a propagation time of seven seconds for a bundle of rays distributed in initial angle from -5 degrees to 10 degrees. The source is located at a depth of 10 yards in an ocean characterized by the velocity profile shown in Fig. IV-2. The data is plotted as ray depth vs initial angle where positive initial angles represent rays with a downward initial direction. The small numbers in brackets represent the number of surface and bottom bounces taken by the rays which comprise each branch of the TIMER plot.

As an example of the application of this data, consider a volume scattering layer located at a depth of 100 yards. Also assume that a round trip propagation time of fourteen seconds is desired. We note that the line drawn across the TIMER plot at a depth of 100 yards intersects the data at five locations. By interpolating between initial angles, a reasonably good estimate may be made of the initial angles required to converge the rays to the 100 yard depth with propagation time seven seconds. A ray plot of these five rays is shown in Fig. IV-3 along with their respective propagation losses in Fig. IV-4. This method is sufficient for the evaluation of the reverberation equation when both the outward and return ray paths are identical. However, when a bistatic situation exists, a somewhat more involved method of evaluating initial angles must be used.

The method described above may be extended to the case of a plane surface at a fixed depth cutting through a number of TIMER plots as shown in Fig. IV-5. If the TIMER tables have been evaluated at close enough intervals, typically one-half second, it will be possible to generate

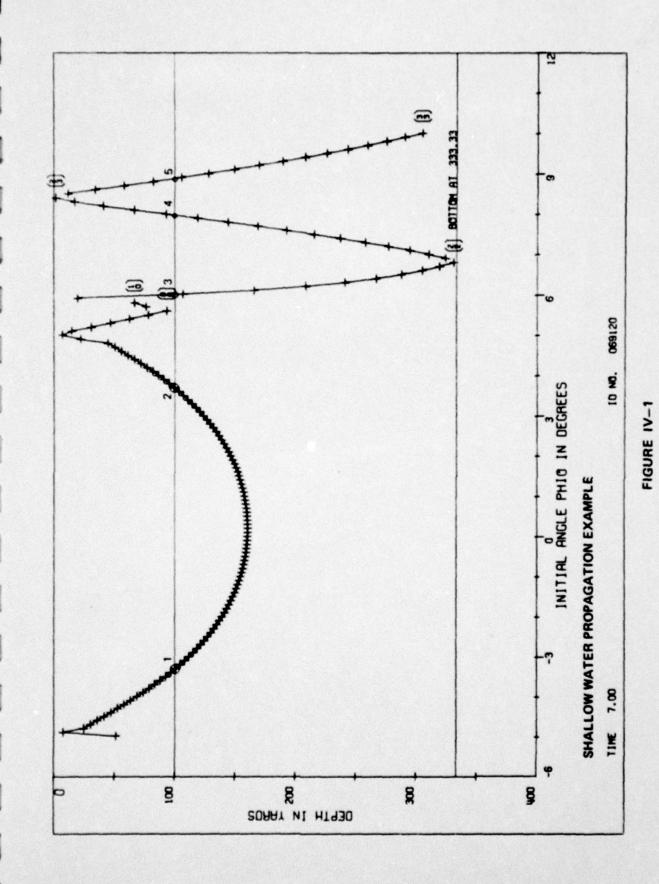lines of initial angles vs propagation time holding the depth fixed.
The fixed depth would of course be the surface or bottom or the
boundaries of a volume scattering layer. This data forms half of the
solution to the bistatic or multipath reverberation problem. However,
we still need a method by which to relate the propagation range to propagation
time, since the bistatic path must be coincident in range and
depth as well as having the same round trip propagation time.

A plot is made of range versus time for the points of intersection
between a constant depth plane and a sequence of TIMER plots. In
Figure IV-6 the rays chosen are the direct rays 1 and 2 of Figure IV-1
and the multibounce ray 5. Assuming that fourteen seconds after transmission
is a time of interest, we may reasonably ask if there is any
combination of dissimilar propagation paths which can return energy to
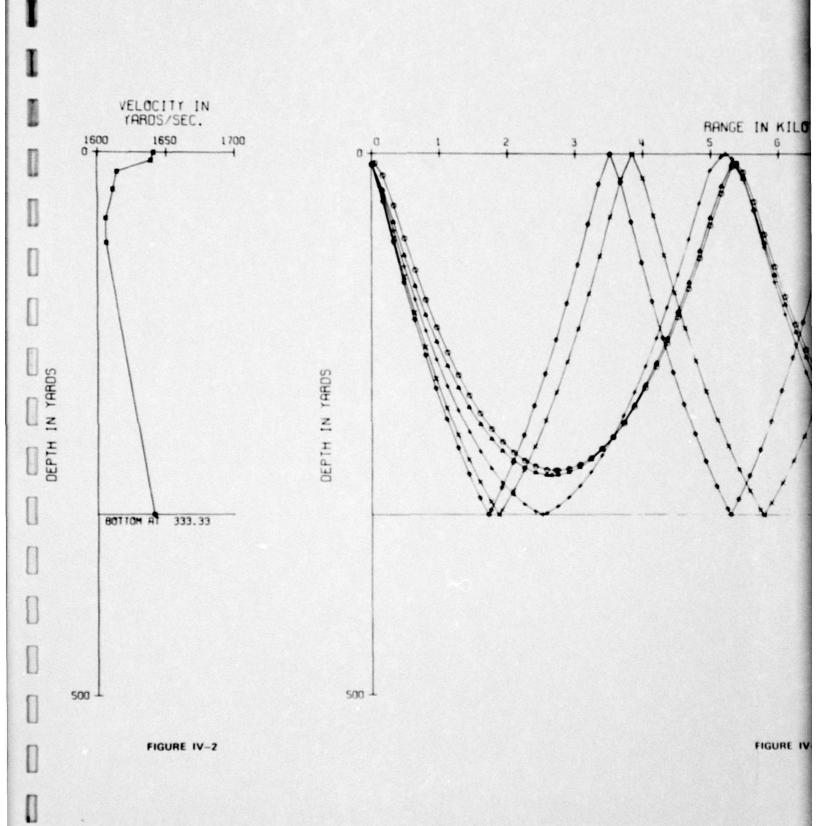the receiver with a total round trip propagation time of fourteen seconds.

From Figure IV-6, it appears that there is indeed such a combination
of paths. The requirement that both paths terminate at the same depth is
satisfied by the cutting of the TIMER plots at a fixed depth. The
requirement that both paths terminate at the same range is satisfied by
constraining the range variable as shown in Figure IV-6. Now, by
adjusting this range variable, R_o, it is possible to find a combination
of propagation times t_1 and t_2 whose sum is the required fourteen seconds.
Knowing the propagation times t_1 and t_2, the final step is to use the
graphs generated by the process shown in Figure IV-5 to obtain
interpolated values for the initial angles of the rays which will fulfill
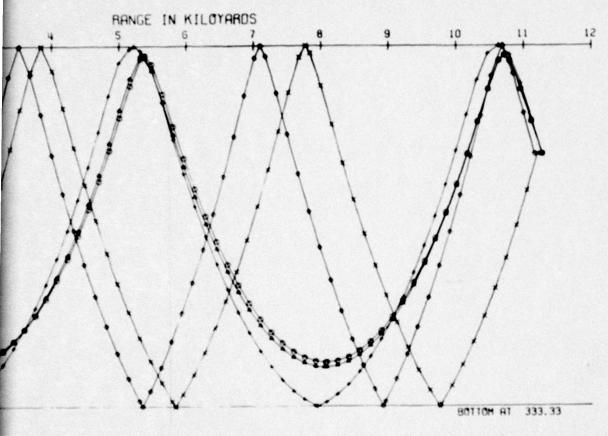the conditions of spatial and temporal coincidence. The result of

this calculation would appear similar to a combination of rays one or two and ray five, as shown in Figure IV-3.

The process of multipath identification and selection has not as yet been integrated into the reverberation program. The programs for doing this task are under development.

SHALLOW WATER PROPAGATION EXAMPLE
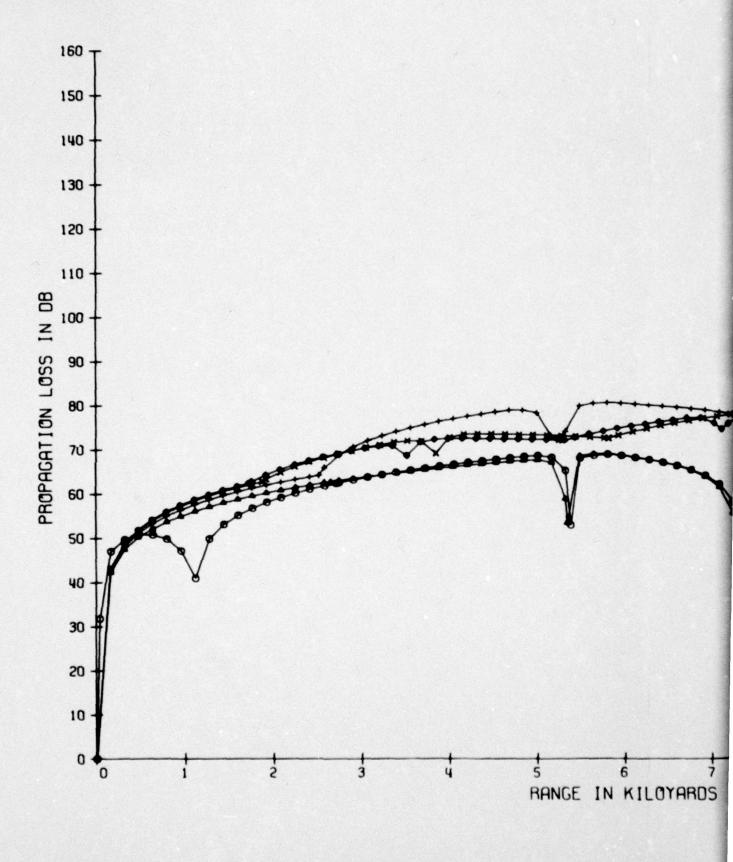
TIME 7.00

INITIAL ANGLE PHI0 IN DEGREES

DEPTH IN YARDS

ID NO. 069120

FIGURE IV-1

VELOCITY IN
YARDS/SEC.

1600   1650   1700

DEPTH IN YARDS

BOTTOM AT   333.33

500

FIGURE IV-2

RANGE IN KILO

0   1   2   3   4   5   6

DEPTH IN YARDS

500

FIGURE IV

1

FIGURE IV-3

FIGURE IV-4

RANGE IN KILOYARDS

FIGURE IV-4
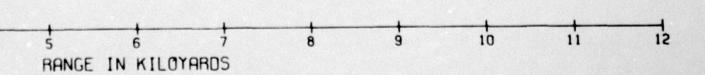
Arthur D Little Inc.
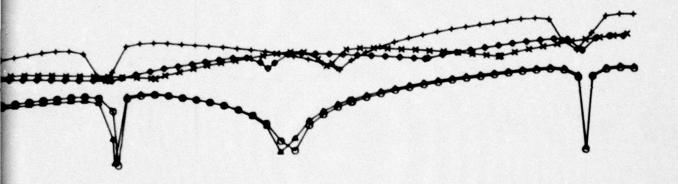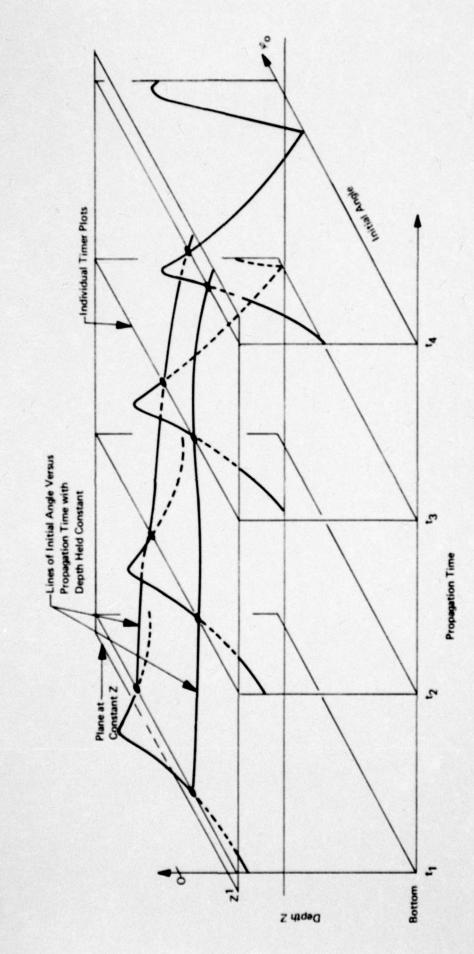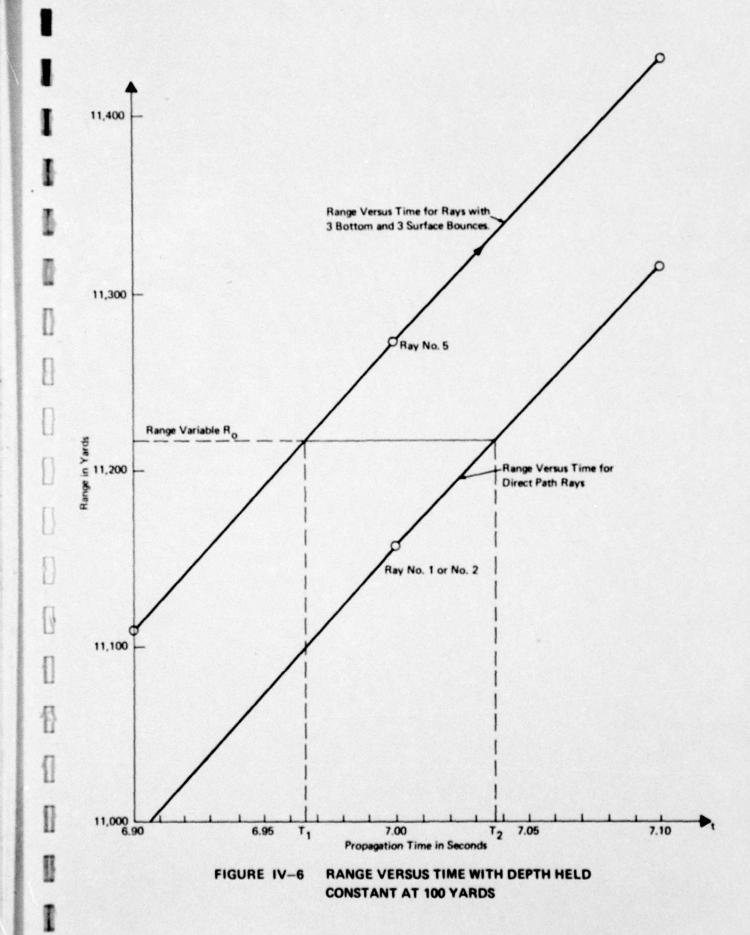
FIGURE IV-5 METHOD OF OBTAINING LINES OF INITIAL ANGLE VERSUS PROPAGATION TIME WITH DEPTH HELD CONSTANT

FIGURE IV–6   RANGE VERSUS TIME WITH DEPTH HELD
CONSTANT AT 100 YARDS

CHAPTER V

ARRAYS AND DOPPLER BROADENING CALCULATIONS

I. Array Calculations

The method used in the reverberation program for the evaluation of the hydrophone array directivity is basically a Fraunhoffer diffraction model. To obtain the particular form of the directivity equation, we start by writing the pressure resulting from a single transducer as

$$P_i(\vec{x}_i, t) = A(|\vec{x}_i|) \exp j \frac{2\pi}{\lambda} (|\vec{x}_i| - ct) \tag{1}$$

where $\vec{x}_i$ is a vector from the ith transducer to the observation point. The function $A(|x_i|)$ is an amplitude factor, λ is the wavelength, c the propagation velocity, and t the time. The total pressure due to an array of N hydrophones is

$$P(t) = \sum_{i=1}^{N} A(|\vec{x}_i|) \exp j \frac{2\pi}{\lambda} (|\vec{x}_i| - ct) \tag{2}$$

At this point we introduce the critical assumption that the distance from a reference point in the hydrophone array, say the ith transducer to the observation point, is much larger than the distance between any two elements in the array. With this assumption we may write that the amplitude functions for any two elements are very nearly equal, since their distances to the observation point are very nearly equal. Thus

$$A(|\vec{x}_i|) = A(|\vec{x}_j|) \tag{3}$$

V-1

and extracting the constant factor exp $j \frac{2\pi}{\lambda} (-ct)$ leaves,

$$P(t) = A(|\vec{x}_o|) \exp(-j \frac{2\pi}{\lambda} ct) \sum_{i=1}^{N} \exp j \frac{2\pi}{\lambda} |\vec{x}_i| \qquad (4)$$

where $\vec{x}_o$ is an average vector from the array to the point of observation.

Let the individual vectors $\vec{x}_i$ be expressed as the sum of the average vector $\vec{x}_o$ and a location vector $\vec{r}_i$ for each element.

$$\vec{x}_i = \vec{x}_o + \vec{r}_i \qquad (5)$$

Also, let $\vec{\ell}$ be a unit vector in the direction of observation, i.e., parallel to the $\vec{x}_o$ vector. Now, using the original assumption that $|\vec{x}_o|$ is much larger than $|r_i|$, we can write the following approximation for the magnitude of $|x_i|$:

$$|\vec{x}_i| = |\vec{x}_o| + \vec{r}_i \cdot \vec{\ell} \qquad (6)$$

Using the result in equation (4) gives

$$P(t) = A(|\vec{x}_o|) \exp j \frac{2\pi}{\lambda} (|\vec{x}_o| - ct) \sum_{i=1}^{N} \exp j \frac{2\pi}{\lambda} (\vec{r}_i \cdot \vec{\ell}) \qquad (7)$$

which we may now place in a more convenient form by normalizing $P(t)$ in the following manner. Define P_{max} as the maximum of equation (4) obtained by holding $|\vec{x}_o|$ constant and varying $\vec{\ell}$ over 4π steradians. Thus in normalized form

$$Q(\vec{\ell}) = \frac{\sum_{i=1}^{N} \exp j \frac{2\pi}{\lambda} (\vec{r}_i \cdot \vec{\ell})}{Q_{max}} \qquad (8)$$

where Q_{max} is the maximum of the summation in the numerator.

It is entirely possible to associate any arbitrary phase with each of the N elements. In particular, suppose that a phase equal to

$$-\frac{2\pi}{\lambda} \vec{r}_i \cdot \vec{m} = \phi_i \tag{9}$$

is associated with each radiator where $\vec{m}$ is a unit vector in some particular direction. Inserting this phase in equation (8) gives

$$Q(\vec{\ell}) = \frac{\sum_{i=1}^{N} \exp j \frac{2\pi}{\lambda} (\vec{r}_i \cdot (\vec{\ell}-\vec{m}))}{N} \tag{10}$$

Clearly, when $\vec{\ell} = \vec{m}$, all the elements are in phase and the summation is maximized such that $Q_{max} = N$. Equation (10) provides a computationally convenient method for accomplishing plane wave phasing.

In addition to an arbitrary phasing, we may also allow an arbitrary weighting function to be applied to each element. For most practical purposes a weighting function dependent on the angle between the observation vector and a unit vector characteristic of the element is sufficiently general. In many cases the unit vector normal to the radiating surface is used as a reference for the weighting function.

Taking into account all of the above consideration, we may write for the general case

$$D(\vec{\ell}) = \frac{\left| \sum_{i=1}^{N} W(\vec{n}_i \cdot \vec{\ell}) \exp j \left[\frac{2\pi}{\lambda} (\vec{r}_i \cdot (\vec{\ell}-\vec{m})) + \phi_i \right] \right|^2}{D_{max}} \tag{11}$$

where the square of $Q(\vec{\ell})$ is used since the directivity is normally associated with power measurements.

To summarize the variables in equation (11) are:

$\vec{n}_i$ unit vector characteristic of the ith transducer.

$\vec{\ell}$ unit vector in the direction of observation.

$W(\vec{n}_i \cdot \vec{\ell})$ weighting function for the ith element.

$\vec{r}_i$ location vector for the ith element.

$\vec{m}$ plane wave phasing unit vector.

ϕ_i arbitrary phasing for the ith element

D_{max} normalizing value equal to the maximum of the
        numerator over all values of $\vec{\ell}$.

As an example of the use of equation (11), we show in Fig. 1 and Fig. 2 the vertical and conical patterns associated with an array of hydrophones having cylindrical symmetry.

II. Doppler Broadening Calculations

The reverberation equation requires the evaluation of a convolution integral of the form

$$\phi(f) = \int_{-\infty}^{\infty} F(\sigma) \, \Lambda(f-\sigma) \, d\sigma \tag{12}$$

where $F(\sigma)$ is a function characteristic of the scatterer motion and

V-4

$\Lambda(f-\sigma)$ is the spectrum of the transmitted signal. In general the repetitive evaluation of this integral by conventional techniques is not feasible. However, by making use of the Fast Fourier Transform (FFT) technique, this calculation may be performed with relative ease. In fact, the use of the FFT greatly simplifies a number of the computational aspects of the reverberation problem.

Before investigating this simplification, we will define the FFT and its inverse and give without proof some elementary but useful properties. The Discrete Fourier Transform (DFT) of a sampled signal of limited bandwidth is defined[1] as

$$F_n = \sum_{k=1}^{N} f_k \exp\left(j \frac{2\pi}{N} nk\right) \tag{13}$$

and the inverse is

$$f_k = \frac{1}{N} \sum_{n=1}^{N} F_n \exp\left(-j \frac{2\pi}{N} nk\right) \tag{14}$$

Using conventional techniques the evaluation of either equation (13) or equation (14) will require N^2 complex operations (i.e., a sine or cosine look up and a multiply). The FFT derives its time savings by capitalizing on the high degree of symmetry of the conversion matrix

$$W(nk) = \exp j \frac{2\pi}{N} nk \tag{15}$$

in order to greatly reduce the number of complex operations required.

[1] The definition of the DFT is not uniform in the literature. Some authors use A_r/N as the DFT coefficients, others use $A_r/\sqrt{N}$, still others use a positive exponent. Cochran, W. T., et al, What is the Fast Fourier Transform? Proc of the IEEE, Vol 55, No. 10, October 1967, p. 1665.

Among the useful properties of the DFT, we have that the time average power in a sample signal $\{f_k\}$ is given by

$$\bar{P} = \sum_{n=1}^{N} F_n F_n^*$$ (16)

In addition, we note that the individual components of the power density spectrum of the sampled function $\{f_k\}$ are

$$P_n = F_n F_n^*$$ (17)

which implies that the autocorrelation function of the signal $\{f_k\}$ may be obtained by inverse transformation of the set of samples $\{P_n\}$. That is

$$\phi_k = \sum_{n=1}^{N} P_n \exp\left(-j \frac{2\pi}{N} nk\right)$$ (18)

Another useful property is that convolution in either frequency or time corresponds to multiplication in the inverse domain. Thus the evaluation of the convolution integral would proceed if done by conventional methods as

$$\phi_n = \sum_{k=1}^{N} G_k \Lambda_{n-k}$$ (19)

However, by making use of the above properties and transforming $\{G_k\}$ and $\{\Lambda_k\}$, we obtain

$$\phi_n = \sum_{k=1}^{N} g_k \lambda_k \exp\left(j \frac{2\pi}{N} nk\right)$$ (20)

which is again evaluated by means of the FFT.

The sequence of operations as used by the program is as follows. The input consists of a time function, $f(t)$, representing the transmitted signal and a set of numerical values representing the variances of the Doppler spreading from both the surface and the volume scatters. The input signal is sampled by a signal generator subroutine to give set of sample values.

$$f(t) \rightarrow \text{sampled} \rightarrow \{f_k\}$$

This set $\{f_k\}$ is then transformed after which the magnitude squared of the transform is obtained.

$$\{f_k\} \rightarrow \text{FFT} \rightarrow \{F_n\}$$

$$\{F_n\} \rightarrow \text{magnitude squared} \rightarrow \{\Lambda_n\}$$

Now the set $\{P_n\}$ is the power density function to be convolved with the scatterer function. Next, we generate the transform of the scatterer characteristic function $\{g_k\}$ which we assume to be gaussian. Following this operation the spectra $\{\Lambda_n\}$ is transformed to give the sampled correlation function $\{\lambda_k\}$.

$$\{\Lambda_n\} \rightarrow \text{inverse FFT} \rightarrow \{\Lambda_k\}$$

Multiplication by the scattering function $\{g_k\}$ followed by a FFT returns the set $\{\phi_n\}$ representing the power density spectra of the Doppler broadened input signal.

V-7

$$\{\lambda_k\} \cdot \{g_k\} \rightarrow \text{multiplication} \rightarrow \{\phi_k\}$$

$$\{\phi_k\} \rightarrow \text{FFT} \rightarrow \{\Phi_n\}$$

Figures 2 through 8 illustrate this sequence of operations for the case of a linear f.m. pulse using the following parameters:

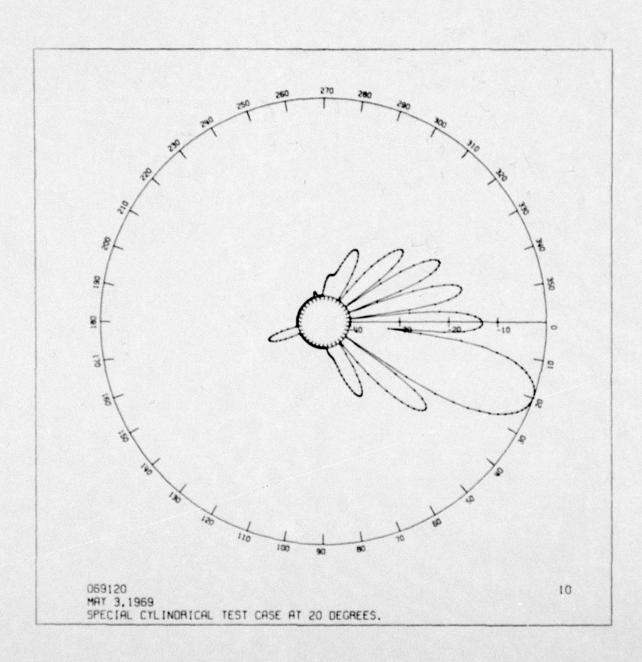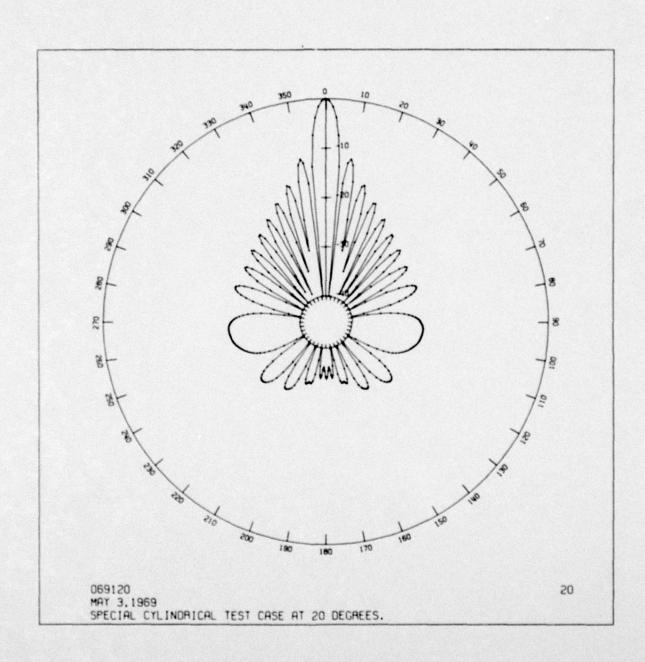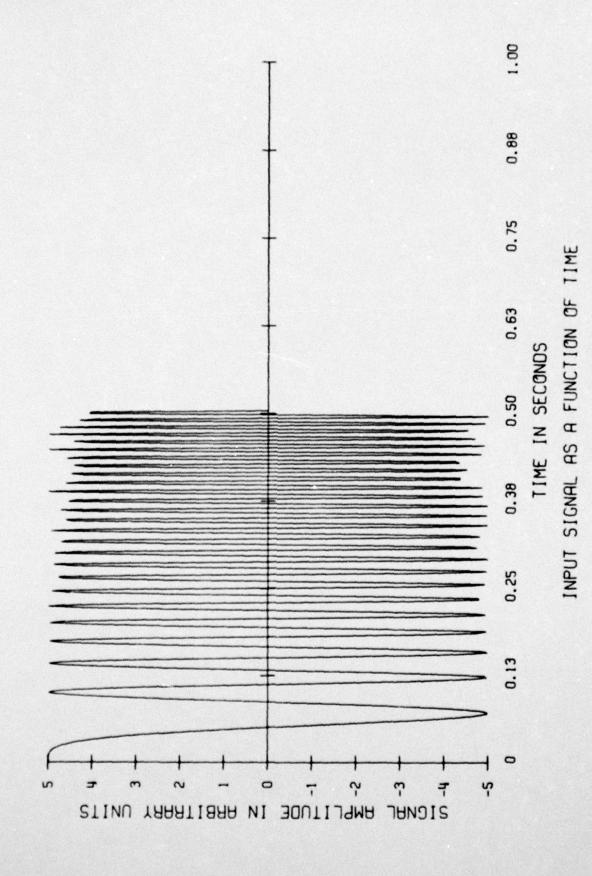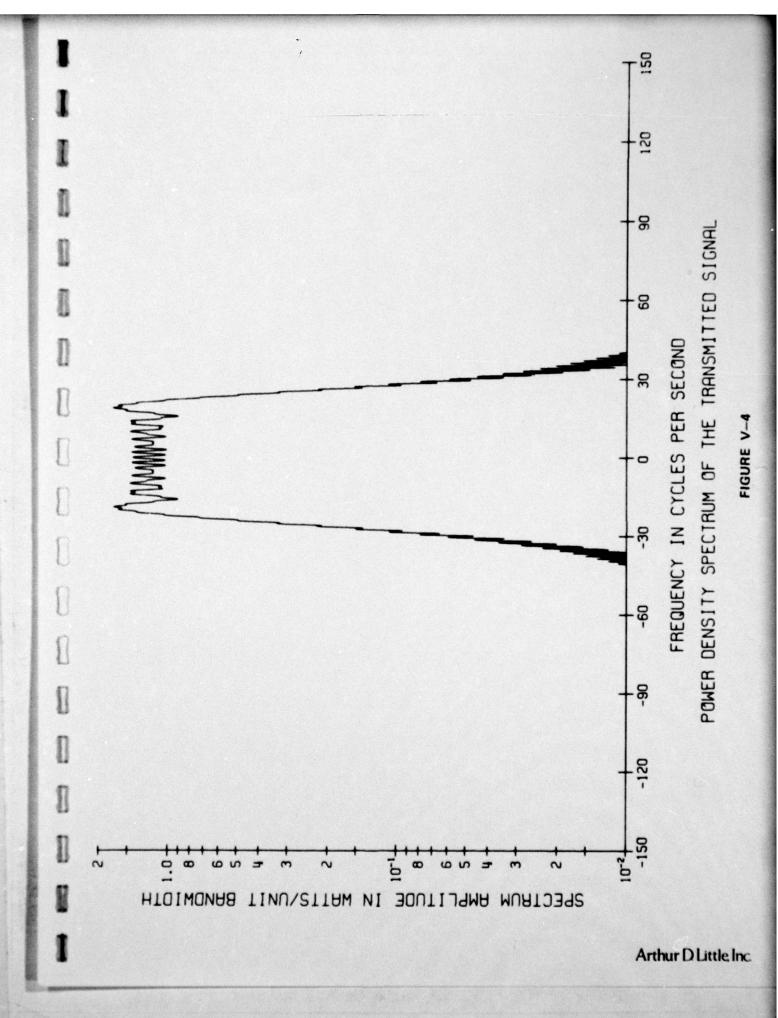|	
sampling interval	0.005 sec.
pulse length	0.50 sec.
repetition rate	1.00 sec.
rate of change of frequency with time	100.0 cps/sec.
total signal bandwidth	100 cycles
bandwidth increment	0.5 cycles

069120
MAY 3, 1969
SPECIAL CYLINDRICAL TEST CASE AT 20 DEGREES.

10

FIGURE V-1

Arthur D Little Inc

20
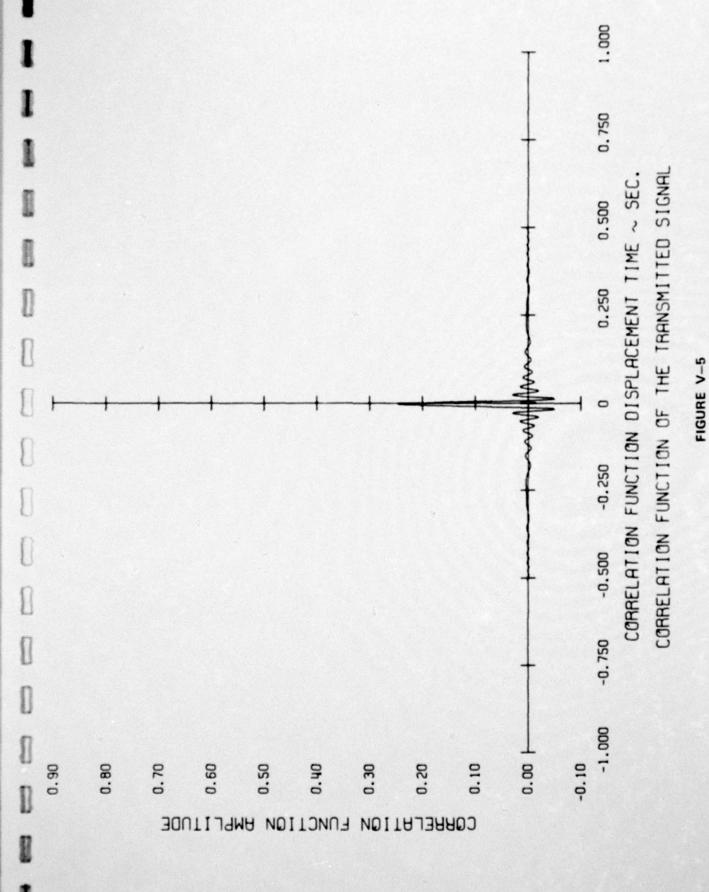
FIGURE V—2

Arthur D Little, Inc.

TIME IN SECONDS

INPUT SIGNAL AS A FUNCTION OF TIME

FIGURE V-3

FREQUENCY IN CYCLES PER SECOND

POWER DENSITY SPECTRUM OF THE TRANSMITTED SIGNAL

FIGURE V-4

Arthur D Little Inc.

CORRELATION FUNCTION DISPLACEMENT TIME ~ SEC.

CORRELATION FUNCTION OF THE TRANSMITTED SIGNAL

FIGURE V-5

Arthur D Little Inc.

CORRELATION FUNCTION DISPLACEMENT TIME ~ SEC.

CHARACTERISTIC FUNCTION FOR DOPPLER BROADENING

FIGURE V-6

Arthur D Little, Inc.

CORRELATION FUNCTION DISPLACEMENT TIME ~ SEC.

PRODUCT OF THE CHACTERISTIC AND CORRELATION FUNCTIONS

FIGURE V-7

FREQUENCY IN CYCLES PER SECOND

POWER DENSITY SPECTRUM OF THE DOPPLER BROADENED SIGNAL
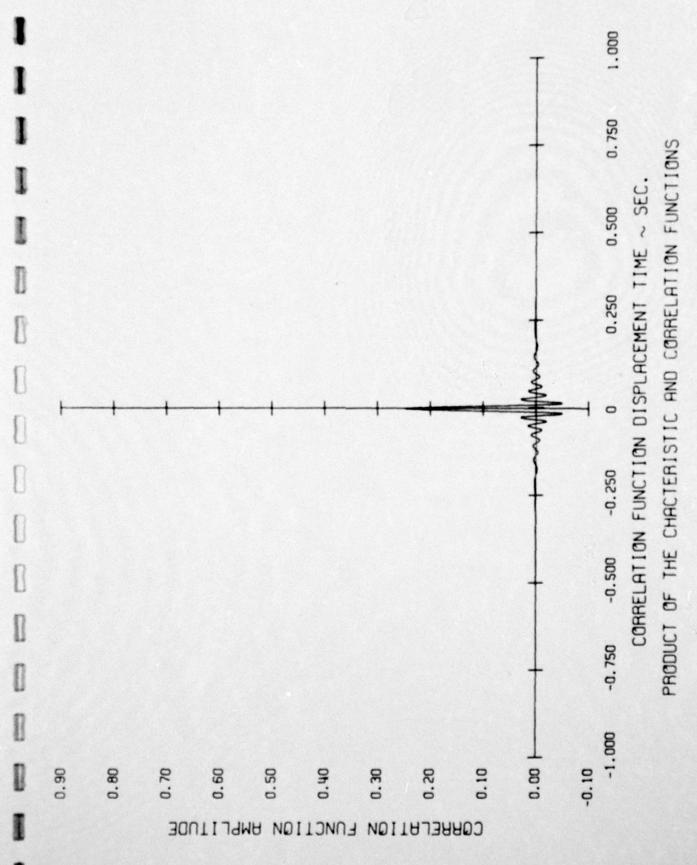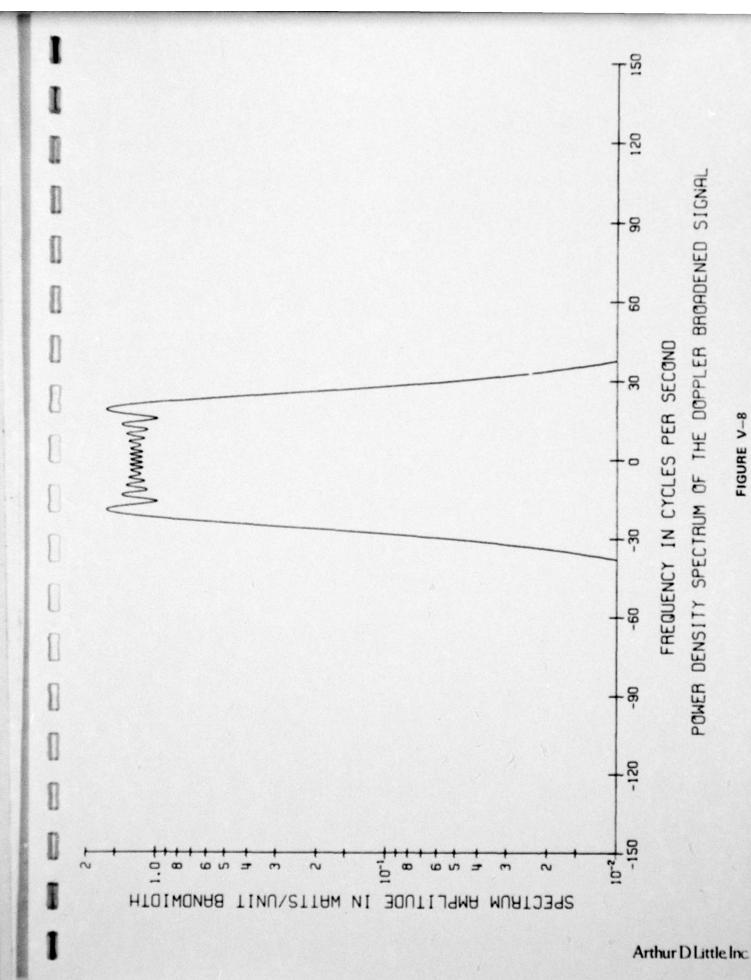
FIGURE V-8

CHAPTER VI

REVERBERATION SPECTRUM COMPUTATION

The reverberation spectrum time history is generated by the program RAND which simply acts as a driver for all of the subroutines described in the preceding chapters. A series of times is chosen at which spectra are desired. Programs TIMER and TIMERP are run for these times with the specified ocean and source depth. From the TIMER plots or printed output initial angles are obtained for each reverberation path (first order surface, first order bottom, etc.) for each time. This step also allows an estimate of the intensity of the selected rays, since the space between points on the TIMER plot is proportional to the spreading loss.

Program RAPID is then run to produce plots of the array directivity. Since RAND has to integrate equation I-40 over all azimuth and depression angles, computation time can be decreased if it is not necessary to integrate over all of the side lobes in detail. Using the RAPID plots one can select integration limits within which the array pattern is computed in detail and outside of which a constant sidelobe level is specified.
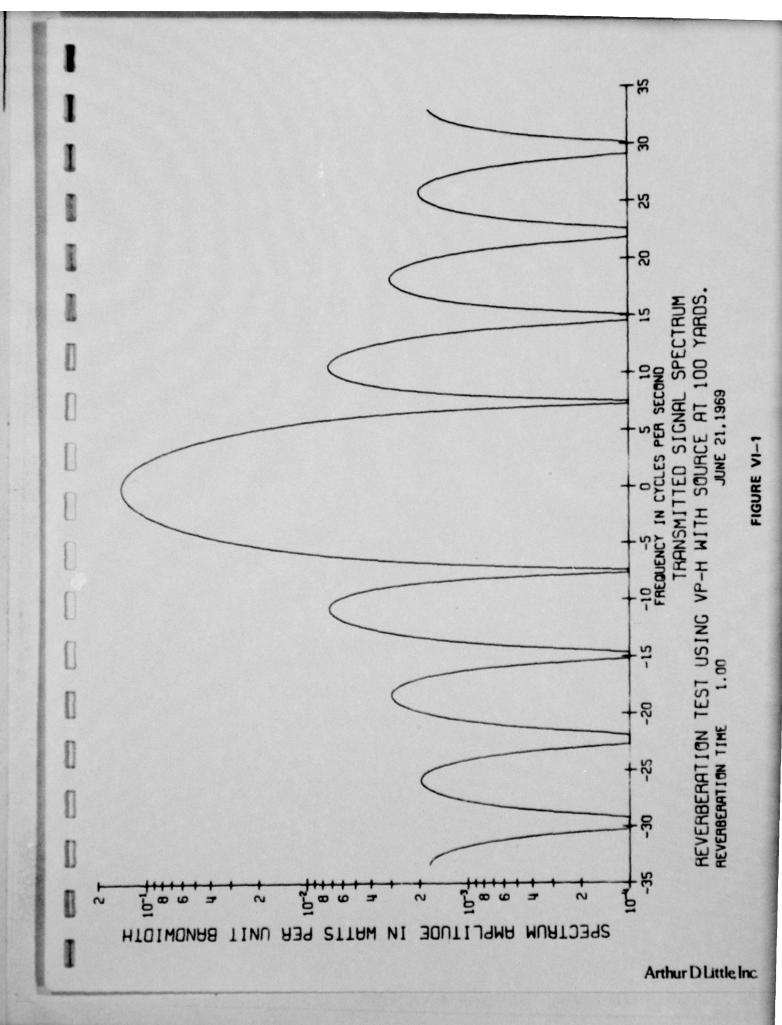
Doppler broadening characteristic functions are specified for program RAND by estimating the bandwidth of the scatterer motion spectrum. The ocean is specified by its velocity profile, the surface by the wind velocity and the bottom by its acoustic province. Two types of transmitted signal are presently available, a pulsed CW signal and a linear FM signal.
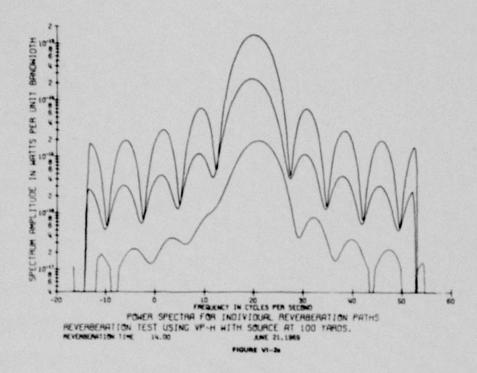
Figures 6.2 and 6.3 show the output of the program for the case of a $\emptyset.125$ second duration CW pulse whose power density spectrum is shown in Figure 6.1. The particular reverberation paths used in this example were determined by examination of the TIMER program output for the one way propagation times of 14.0 and 15.0 seconds. Within the depression angle range considered, it was found that three ray paths existed for the 14 second case and four paths existed for the 15 second case. The first three paths consisted of: 1) direct to the bottom, 2) one bottom bounce and terminating in a scattering layer, and 3) one bottom bounce and terminating on the surface. The 15 second time allowed one additional path consisting of one bottom bounce, one surface bounce and termination in the scattering layer. The initial angles of each of these rays now formed the basic input for each reverberation time.

The transducer array used in this example was depressed an angle of 30° and the following doppler broadenings were assumed for the various scatterers:

ship	1 cps rms
surface	2 cps rms
volume	4 cps rms

For this particular example it happens that the first path, direct to the bottom and back, is dominant. For other times, oceans, arrays and depression angles, the dominant reverberation may come from a less obvious path. The RAND program allows a systematic investigation of the effect on reverberation of sonar and ship operating parameters.

Arthur D. Little, Inc.

REVERBERATION TEST USING VP-H WITH SOURCE AT 100 YARDS.

REVERBERATION TIME   1.00   JUNE 21,1969

FIGURE VI-1

TRANSMITTED SIGNAL SPECTRUM

FREQUENCY IN CYCLES PER SECOND

SPECTRUM AMPLITUDE IN WATTS PER UNIT BANDWIDTH

Arthur D Little Inc

SPECTRUM AMPLITUDE IN WATTS PER UNIT BANDWIDTH

FREQUENCY IN CYCLES PER SECOND

POWER SPECTRA FOR INDIVIDUAL REVERBERATION PATHS
REVERBERATION TEST USING VP-H WITH SOURCE AT 100 YARDS.
REVERBERATION TIME   14.00   JUNE 21,1969

FIGURE VI-2a

SPECTRUM AMPLITUDE IN WATTS PER UNIT BANDWIDTH

FREQUENCY IN CYCLES PER SECOND

TOTAL REVERBERATION POWER DENSITY SPECTRUM
REVERBERATION TEST USING VP-H WITH SOURCE AT 100 YARDS.
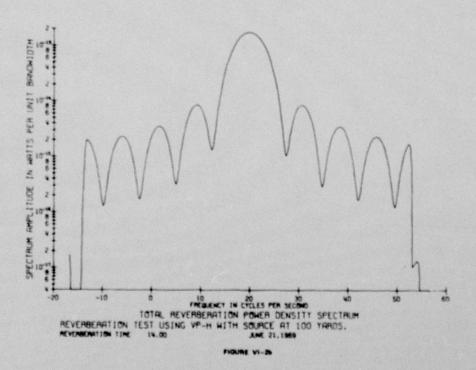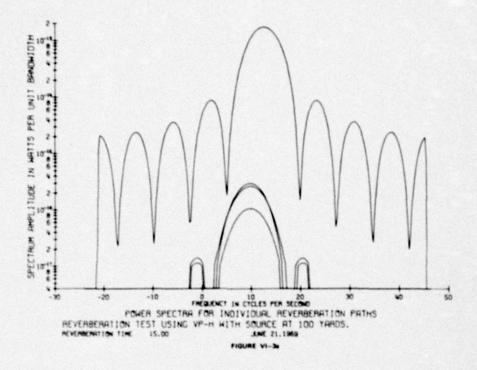REVERBERATION TIME   14.00   JUNE 21,1969

FIGURE VI-2b

FIGURE VI-2   SPECTRA FROM INDIVIDUAL REVERBERATION PATHS
AND TOTAL POWER SPECTRA FOR ROUND TRIP
PROPAGATION TIME OF 28 SECONDS

POWER SPECTRA FOR INDIVIDUAL REVERBERATION PATHS
REVERBERATION TEST USING VP-H WITH SOURCE AT 100 YARDS.
REVERBERATION TIME 15.00 JUNE 21,1969
FIGURE VI-3a

TOTAL REVERBERATION POWER DENSITY SPECTRUM
REVERBERATION TEST USING VP-H WITH SOURCE AT 100 YARDS.
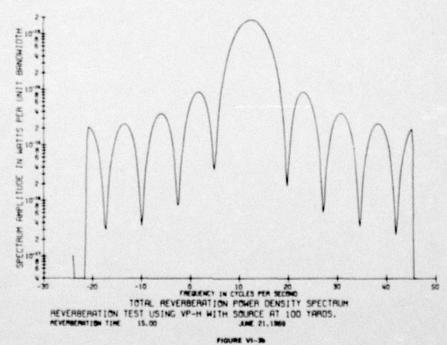REVERBERATION TIME 15.00 JUNE 21,1969
FIGURE VI-3b

FIGURE VI-3   SPECTRA FROM INDIVIDUAL REVERBERATION PATHS
AND TOTAL POWER SPECTRA FOR ROUND TRIP
PROPAGATION TIME OF 30 SECONDS